MOLECULAR AND CELLULAR BIOLOGY, May 2007, p. 3441–3455 Vol. 27, No. 9
0270-7306/07/$08.00+0 doi:10.1128/MCB.01643-06

mRNAs Encoding Polarity and Exocytosis Factors Are Cotransported with the Cortical Endoplasmic Reticulum to the Incipient Bud in *Saccharomyces cerevisiae*▽†

Stella Aronov,‡ Rita Gelin-Licht,‡ Gadi Zipor, Liora Haim, Einat Safran, and Jeffrey E. Gerst*

Department of Molecular Genetics, Weizmann Institute of Science, Rehovot 76100, Israel

Received 3 September 2006/Returned for modification 13 November 2006/Accepted 9 February 2007

Polarized growth in the budding yeast *Saccharomyces cerevisiae* depends upon the asymmetric localization and enrichment of polarity and secretion factors at the membrane prior to budding. We examined how these factors (i.e., Cdc42, Sec4, and Sro7) reach the bud site and found that their respective mRNAs localize to the tip of the incipient bud prior to nuclear division. Asymmetric mRNA localization depends upon factors that facilitate *ASH1* mRNA localization (e.g., the 3′ untranslated region, She proteins 1 to 5, Puf6, actin cytoskeleton, and a physical association with She2). mRNA placement precedes protein enrichment and subsequent bud emergence, implying that mRNA localization contributes to polarization. Correspondingly, mRNAs encoding proteins which are not asymmetrically distributed (i.e., Snc1, Mso1, Tub1, Pex3, and Oxa1) are not polarized. Finally, mutations which affect cortical endoplasmic reticulum (ER) entry and anchoring in the bud (*myo4*Δ, *sec3*Δ, and *srp101*) also affect asymmetric mRNA localization. Bud-localized mRNAs, including *ASH1*, were found to cofractionate with ER microsomes in a She2- and Sec3-dependent manner; thus, asymmetric mRNA transport and cortical ER inheritance are connected processes in yeast.

The establishment and maintenance of cell polarity in eukaryotes require coordination of the cell cycle, actin and microtubule cytoskeletons, and the secretory pathway to regulate growth along a given axis (9, 19, 38, 49). Asymmetric cell growth is necessary for a variety of cellular processes, including division (3, 6, 34), axon extension (29), motility (30, 51), and body morphogenesis (3, 24, 66). Polarization necessitates a role for polarity factors that are capable of regulating the cell cycle, cytoskeleton, and the secretory pathway but that are also responsive to extracellular signals (i.e., chemotactic signals, pheromones, and cell-cell contacts) in order to promote directed growth. Small GTPases of the Rho family (i.e., Cdc42 and Rho) have a conserved role in evolution as being master regulators of polarity (31, 49). In the budding yeast, *Saccharomyces cerevisiae*, polarized growth processes (e.g., budding and mating) require Cdc42 activation, which is necessary for polarization of the actin cytoskeleton (13, 31, 49). During budding, the commitment to polarize occurs during the G_1 phase of the cell-cycle and leads to the formation of a cap of activated Cdc42 at the presumptive bud site. This asymmetric clustering of Cdc42 is sufficient to induce actin polymerization and subsequent polarization (32, 53, 61). Spatial regulation of the Cdc42 cap formation is aided by the existence of landmark proteins (or anchors) which enhance selection of a given bud site, usually adjacent to the previous bud scar in haploid cells (13, 54). However, regulation of the local Cdc42 concentration is sufficient to induce and maintain polarization (32, 53, 61). In G_1-arrested unbudded cells, as well as cells lacking either landmarks or polarized actin, Cdc42 can become polarized and induce directed growth (32, 61). Recent work also suggests a role for endocytosis and protein recycling in maintenance of the Cdc42 cap in newly forming buds (33). In addition to Cdc42, other polarity and secretion factors (POLs) concentrate at the presumptive bud site and incipient bud, including components of the exocyst (e.g., Sec3, Sec5, Sec6, Sec8, Sec10, Sec15, Exo70, and Exo84), Rho and Sec4 GTPases, Sec1, Myo2, and others (9, 27, 34, 50). Maintenance of their local concentrations may involve endocytosis, as suggested for v-SNARE recycling within the bud (59), although many of these proteins are soluble and have no direct means to target to the endocytic pathway.

Other studies suggest a role for mRNA localization as a means of regulating the local concentration of proteins. For example, the asymmetric localization of *ASH1* mRNA to the bud restricts the localization of Ash1 protein in order to regulate mating type switching in yeast (42, 57). In higher eukaryotes, mRNA localization regulates embryonic patterning in *Drosophila*, as well as the subcellular localization of axonal proteins in neurons and β-actin in motile cells (15, 38, 66). *ASH1* mRNA trafficking in yeast depends upon the *SHE1*/*MYO4* and *SHE2-5* genes, an intact secretory pathway, and in part upon its 3′ untranslated region (UTR). *SHE1*/*MYO4* encodes a type V myosin that mediates *ASH1* mRNA transport along actin filaments (35). *SHE2* encodes an mRNA binding protein, and *SHE3* encodes the adaptor that connects She2 to She1/Myo4 (7, 44, 58). *SHE4* encodes a protein involved in actin-dependent endocytosis (62), and *SHE5* encodes a formin ortholog involved in actin regulation (21). In our studies, we found that *ASH1* mRNA localization depends upon the integrity of the secretory pathway,

* Corresponding author. Mailing address: Department of Molecular Genetics, Weizmann Institute of Science, Rehovot 76100, Israel. Fax: 972 8 9344108. Phone: 972 8 9342106. E-mail: jeffrey.gerst@weizmann.ac.il.

‡ S.A. and R.G.-L. contributed equally to this study.

† Supplemental material for this article may be found at http://mcb.asm.org/.

▽ Published ahead of print on 5 March 2007.

TABLE 1. Yeast strains

Strain	Genotype	Source
W303-1a	*MAT***a** *ade2 can1 his3 leu2 lys2 trp1 ura3*	J. Hirsch
W303-1b	*MATα ade2 can1 his3 leu2 lys2 trp1 ura3*	J. Hirsch
NY1002	*MATα his3 leu2 trp1 ura3 myo2−66*	P. Novick
BY4741	*MAT***a** *his3Δ1 leu2Δ0 met15Δ0 ura3Δ0*	Euroscarf
*myo4*Δ	*MAT***a** *his3Δ1 leu2Δ0 met15Δ0 ura3Δ0 myo4*Δ*::kanMX*	Euroscarf
*puf6*Δ	*MAT***a** *his3Δ1 leu2Δ0 met15Δ0 ura3Δ0 puf6*Δ*::kanMX*	Euroscarf
*she2*Δ	*MAT***a** *his3Δ1 leu2Δ0 met15Δ0 ura3Δ0 she2*Δ*::kanMX*	Euroscarf
*she3*Δ	*MAT***a** *his3Δ1 leu2Δ0 met15Δ0 ura3Δ0 she3*Δ*::kanMX*	Euroscarf
*she4*Δ	*MAT***a** *his3Δ1 leu2Δ0 met15Δ0 ura3Δ0 she4*Δ*::kanMX*	Euroscarf
*she5*Δ	*MAT***a** *his3Δ1 leu2Δ0 met15Δ0 ura3Δ0 she5*Δ*::kanMX*	Euroscarf
NY2450	*MAT***a** *his3Δ200 leu2-3,112 ura3-5 sec3*Δ*::kanMX4*	P. Novick
RGY1	*MAT***a** *his3Δ1 leu2Δ0 met15Δ0 ura3Δ0 she2*Δ*::kanMX sro7::his5+::GAL1-GFP-SRO7*	This study
RGY2	*MAT***a**/*α ade2/ADE2 can1/CAN1 his3/his3Δ1 leu2/leu2Δ0 lys2/LYS2 MET15/met15Δ0 ura3/ura3Δ0 SHE2/she2*Δ*::kanMX SRO7/sro7::his5+::GAL1-GFP-SRO7*	This study
WPY154	*MATα ura3-52 his3Δ200 leu2Δ1 srp101-47*	W. Prinz

suggesting a connection between the processes of mRNA transport and exocytosis (1).

We postulated that the local enrichment of POLs in the incipient bud might be due to targeted mRNA delivery to the presumptive bud site and subsequent local translation. By examining the localization of POL mRNAs and proteins in situ and in vivo, we found that mRNA localization precedes local protein enrichment and subsequent bud emergence. mRNAs encoding bud-localized POLs (e.g., *CDC42*, *SEC4*, and *SRO7*) localize asymmetrically to the tip of the emerging bud in a manner dependent upon their 3′ UTRs, She1-5, Puf6, Myo2, and She2-binding. Bud enrichment of a nonanchored POL, Sro7, was mRNA transport dependent while that of membrane-anchored factors (e.g., Cdc42 and Sec4) was mRNA transport independent. We propose that mRNA transport plays an important role in the bud enrichment of proteins that lack membrane-anchoring signals and that asymmetric POL mRNA localization may facilitate polarization.

As Myo4 and She3 are required for both asymmetric mRNA transport and the retention of cortical endoplasmic reticulum (ER) in the early bud (ER inheritance) (20, 63, 64), we examined whether these processes are connected. We found that POL mRNA localization to the tip of the emerging bud correlated directly with the presence of the cortical ER. Correspondingly, a mutation in *SEC3*, which encodes an exocyst component involved in exocytosis (27) and ER inheritance (64), blocked asymmetric mRNA localization. Finally, cell fractionation studies demonstrated the cofractionation of *ASH1* and bud-localized POL mRNAs with ER microsomes in a She2- and Sec3-dependent manner. Thus, asymmetric mRNA localization and ER inheritance are connected. This may ensure that membrane proteins encoded by bud-localized mRNAs can undergo translocation upon translation, as well as to spatially restrict the translation of soluble proteins.

MATERIALS AND METHODS

Media, yeast, cell culture, and imaging. Yeast cells were typically grown to mid-log phase in standard synthetic or rich (yeast extract, peptone, and dextrose) growth medium containing 2% glucose as a carbon source. For the galactose-inducible *RFP-SRO7* construct, wild-type (WT) cells were grown in raffinose-containing synthetic medium prior to the shifting of cells to medium containing galactose (3.5%). For the galactose-inducible integrated *GFP-SRO7*, cells were shifted to galactose-containing medium for 6 to 14 h. Strains are listed in Table 1. Cells transformed with plasmids for fluorescent protein expression were grown on selective medium. For the induction of MS2 fused to green fluorescent protein (MS2-GFP), cells were switched to medium lacking methionine for 1.5 h at 26°C, with the exception of *myo2-66* cells, which were induced for 2.5 h at either 26°C or 37°C. Cells were taken directly for live cell imaging by fluorescence or confocal microscopy. To obtain quantitative data on the localization of mRNA and red fluorescent protein (RFP) in each strain examined, cells with small visible buds (i.e., cells in S and early G_2/M phase) were scored for the localization of GFP (mRNA) and RFP (protein) signals. The following wavelengths were used: for GFP, excitation at 480 nm and emission at 530 nm; for rhodamine or monomeric RFP, excitation at 545 nm and emission at 560 to 580 nm. Cells having mRNA granules in both the tip of the daughter cell, as well as in the mother cell, were scored as having bud tip-localized mRNA.

Plasmids. Plasmids encoding an *ASH1* gene fragment with MS2 viral coat protein binding sites in its 3′ UTR (pIIIA/ASH1-UTR) and a gene fusion of the MS2 coat protein and GFP (pCP-GFP) (4) were generously provided by Kerry Bloom (University of North Carolina, NC). A plasmid, pSL1180, which encodes 12 loops of the viral MS2 coat protein binding site was generously provided by Robert Singer (Albert Einstein College of Medicine, NY). A multicopy plasmid expressing Sec63-RFP, pSM1960, was generously provided by S. Michaelis (John Hopkins, Baltimore, MD). pAD6 is a multicopy expression vector containing the *LEU2* marker and encodes the myc epitope downstream of the *ADH1* promoter. Plasmids used in this study are listed in Table 2. An integration construct, pFA6a-His3MX6-PGAL1-GFP (43), was used along with a specific oligonucleotide pair to *SRO7* in order to generate a *GAL1-GFP-SRO7* integration at the *SRO7* locus. Integration was verified by PCR analysis.

FISH and immunofluorescence. mRNAs were detected by fluorescence in situ hybridization (FISH), as described previously (1). RNAs were synthesized using PCR-amplified DNA fragments of the appropriate genes as templates. The templates included the following: *CDC42* (bp 1 to 600), *RHO3* (1 to 696), *YPT1* (1 to 621), *SEC1* (1 to 648), *SEC4* (1 to 530), *EXO84* (1 to 400), *SEC3* (1 to 480), *TUB1* (1 to 550), *SRO7* (1 to 400), *SRO77* (1 to 480), *SSO1* (1 to 280), and *SNC1* (1 to 310). RNA probes were synthesized in sense and antisense orientations, using a digoxigenin RNA labeling kit (Roche, Mannheim, Germany). After hybridization, cells were washed in 0.2× SSC (1× SSC is 0.15 M NaCl plus 0.015 M sodium citrate) and blocked in 1× phosphate-buffered saline containing 0.1% Triton X-100 and 10% horse serum. Cells were incubated with horseradish peroxidase-conjugated antidigoxigenin monoclonal antibodies (1:500) (Jackson ImmunoResearch, West Grove, PA) in blocking buffer for 2 h. After a washing step, cells were incubated with Cy5-conjugated anti-horseradish peroxidase antibodies (1:100) (Jackson ImmunoResearch) for 2 h at room temperature. Cells were then washed and mounted in 0.01 M Tris-Cl, pH 8.4, 90% glycerol, 1 mg/ml *p*-phenylenediamine, and 0.1 μg/ml propidium iodide (Sigma, St. Louis, MO).

Fluorescence imaging was performed using a Zeiss laser scanning confocal microscope. The following wavelengths were used: for rhodamine-phalloidin, excitation at 545 nm and emission at 560 to 580 nm; for Cy5, excitation at 650 nm and emission at 680 nm. Control experiments for in situ hybridization showed no observable background using the sense RNA probes. No signal was observed in the absence of primary antibodies. To obtain quantitative data on mRNA localization in each strain, between 80 to 120 cells with visible small buds (i.e., cells

TABLE 2. Plasmids created for this study

Plasmid name[a]	Gene	Backbone	Sites[b]	Type	Selectable marker	Source
pAD54-**SRO7**	SRO7	pAD54	SalI-SmaI	2μm	*LEU2*	This study
pAD54-RFP-**SRO7**	*RFP*[c]	pAD54-SRO7	SalI-SalI	2μm	*LEU2*	This study
pAD54-**SRO7**-MS2	*MS2*[d]	pAD54-SRO7	SmaI	2μm	*LEU2*	This study
pAD54-**SRO7**-3′UTR	*SRO7-3′-UTR* (+500 bp)[e]	pAD54	SalI-SmaI	2μm	*LEU2*	This study
pAD54-RFP-**SRO7**-3′ UTR	*RFP*[c]	pAD54-SRO7-3′ UTR	SalI-SalI	2μm	*LEU2*	This study
pAD54-MS2-**SRO7**-3′ UTR	*MS2*[d]	pAD54-SRO7-3′ UTR	[HindIII]	2μm	*LEU2*	This study
pAD54-RFP-**SRO7**-MS2-3′ UTR	*MS2-3′-UTR*^{SRO7} (+500 bp)[e]	pAD54-RFP-SRO7	SmaI-SacI	2μm	*LEU2*	This study
pGAL-RFP-**SRO7**-MS2-3′ UTR	*RFP-SRO7-MS2-3′-UTR*[f]	pYES2	HindIII	2μm	*URA3*	This study
pAD54-**SEC4**	SEC4	pAD54	SalI-SacI	2μm	*LEU2*	This study
pAD54-RFP-**SEC4**	*RFP*[c]	pAD54-SEC4	SalI-SalI	2μm	*LEU2*	This study
pAD54-**SEC4**-MS2	*MS2*[d]	pAD54-SEC4	SmaI	2μm	*LEU2*	This study
pAD54-**SEC4**-3′ UTRs[g]	*3-UTR*^{SEC4} (+136 bp)[e]	pAD54-SEC4	SalI-Sma1	2μm	*LEU2*	This study
pAD54-RFP-**SEC4**-3′ UTRs[g]	*RFP*[c]	pAD54-Sec4-3′ UTRs	SalI-Sal1	2μm	*LEU2*	This study
pAD54-MS2-**SEC4**-3′ UTRs[g]	*MS2*[d]	pAD54-SEC4-3′ UTRs	[SalI]	2μm	*LEU2*	This study
pAD54-RFP-**SEC4**-MS2-3′ UTR	*MS2-3′-UTR*^{SEC4} (+358 bp)[e]	pAD54-RFP-SEC4	[SacI]	2μm	*LEU2*	This study
pAD54-RFP-**SEC4AA**-MS2-3′ UTR	*SEC4*$^{A214/A215}$	pAD54-RFP-SEC4-MS2-3′ UTR		2μm	*LEU2*	This study
pAD54-**CDC42**	*CDC42*	pAD54	SalI-SmaI	2μm	*LEU2*	This study
pAD54-RFP-**CDC42**	*RFP*[c]	pAD54-CDC42	SalI-SalI	2μm	*LEU2*	This study
pAD54-**CDC42**-MS2	*MS2*[d]	pAD54-CDC42	SmaI	2μm	*LEU2*	This study
pAD54-RFP-**CDC42**-MS2-3′ UTR	*MS2-3′-UTR*^{CDC42} (+435 bp)[e]	pAD54-RFP-CDC42-3′ UTR	SmaI-SacI	2μm	*LEU2*	This study
pAD54-**SNC1**-MS2	*MS2*[d]	pAD54-RFP-cSNC1	[SacI]	2μm	*LEU2*	This study
pAD54-RFP-**SNC1**-MS2-3′ UTR	*MS2-3′-UTR*^{SNC1} (+285 bp)[e]	pAD54-RFP-cSNC1	[SacI]	2μm	*LEU2*	This study
pAD54-RFP-MS2	*MS2*[d]	pADH54-RFP	SmaI	2μm	*LEU2*	This study
pAD54-**PEX3**	*PEX3*	pAD54	SalI-SmaI	2μm	*LEU2*	This study
pAD54-**PEX3**-MS2-3′ UTR	*MS2-3′-UTR*^{PEX3} (+474 bp)[e]	pAD54-PEX3	SacI	2μm	*LEU2*	This study
pAD4Δ-**OXA1**[h]	*OXA1*	pAD4Δ	SalI-SmaI	2μm	*LEU2*	This study
pAD4Δ-**OXA1**-RFP[h]	*RFP* (without ATG)	pAD4Δ-OXA1	SmaI-SacI	2μm	*LEU2*	This study
pAD4Δ-**OXA1**-RFP-MS2-3′ UTR[h]	*MS2-3′-UTR*^{OXA3} (+500 bp)[e]	pAD4Δ-OXA1-RFP	SacI	2μm	*LEU2*	This study
pMET-RFP-**MSO1**-MS2-3′ UTR-MSO1[h]	*RFP-MSO1-MS2-3′-UTR*^{MSO1} (+447 bp)[e]	pUG36[i]	SmaI-SpeI[k]	*CEN*	*URA3*	This study
pAD6-myc-SHE2-3′ UTRshort	*SHE2-3′-UTR* (+40 bp)[e]	pAD6	SalI-SacI	2μm	*LEU2*	This study
pCP-GFP	*MS2-GFP*			*CEN*	*HIS3*	K. Bloom
pIIIA/ASH1-3′ UTR	*3′-UTR*^{ASH1}			2μm	*URA3*	K. Bloom
pSL-MS2-12X	*MS2*[d] (12 loops)					R. Singer
pSL-MS2-3′ UTR-**SRO7**	*3′-UTR*^{SRO7} (500 bp)	pSL-MS2-12	SacI-BglII			This study
pSL-MS2-3′ UTR-**SEC4**	*3′-UTR*^{SEC4} (358 bp)	pSL-MS2-12	SacI-[BglII]			This study
pSL-MS2-3′ UTR-**CDC42**	*3′-UTR*^{CDC42} (435 bp)	pSL-MS2-12	SacI-BglII			This study
pSL-MS2-3′ UTR-**OXA1**	*3′-UTR*^{OXA1} (500 bp)	pSL-MS2-12Sac[j]	BglII-SacI			This study
pSL-MS2-3′ UTR-**PEX3**	*3′-UTR*^{PEX3} (474 bp)	pSL-MS2-12Sac[j]	BglII-SacI			This study
pSL-MS2-3′ UTR-**MSO1**	*3′-UTR*^{MSO1} (447 bp)	pSL-MS2-12	BglII-SacI			This study

[a] POL of interest is in boldface.
[b] Brackets indicate blunt-end ligation.
[c] Without ATG and termination codons.
[d] Indicates MS2 binding sites (12 copies).
[e] Indicates length of 3′ UTR.
[f] Amplified by PCR and subcloned.
[g] Short 3′ UTR.
[h] These constructs lack the HA epitope at the amino terminus.
[i] GFP was removed and the XbaI site was destroyed by fill-in and self-ligation.
[j] Indicates addition of a SacI site 5′ to the MS2 loop sequences by *Pfu* site-directed mutagenesis.
[k] A [PaeI]/SpeI fragment containing the *RFP-MSO1-MS2-3′-UTR* cassette was created first in pAD54, amplified by PCR, transferred to pGEM-Teasy, and then cloned into these sites.

in G_1/S and early G_2/M phase) were scored for the localization of mRNA signals using FISH. The data are summarized in Fig. 1.

Immunoprecipitation of She2 and mRNA detection by reverse transcription-PCR (RT-PCR). WT yeast cells (W303-1a) containing either pAD6 or pADH-myc-She2 were grown on synthetic medium to an optical density at 600 nm (OD_{600}) of 1, centrifuged at 3,000 × *g* for 5 min at 4°C, and resuspended in 100 OD_{600} units per ml in lysis buffer (25 mM HEPES-KOH, pH 7.5, 150 mM KCl, 2 mM $MgCl_2$, 100 U/ml RNasin [Promega], 0.1% NP-40, 1 mM dithiothreitol, 100 μM vanadyl complex, 2 μg/ml aprotinin, 1 μg/ml pepstatin, 0.5 μg/ml leupeptin, and 0.01 μg/ml benzamidine). Cells (at a density of 100 OD_{600} units) were broken by vortexing with glass beads (0.5 mm) at 4°C and centrifuged at 4,000 × *g* for 10 min at 4°C. For immunoprecipitation (IP) and Western analysis, 500 μg of protein of the supernatant diluted in lysis buffer (final volume, 0.5 ml) was subjected to IP with 1 μg of anti-myc antibody (Roche) and detection with the same antibody (1:1,000 dilution) following immunoblotting. For IP and RNA extraction experiments, 200 μl of lysate (representing 20 OD_{600} units of cells) was incubated with 5 μg of anti-myc antibody for 2 h at 4°C with rotation, after which 50 μl of protein A-G agarose slurry was added and incubated for an additional 2 h at 4°C. The agarose beads were then washed (three times) with wash buffer (25 mM HEPES-KOH, pH 7.5, 150 mM KCl, 2 mM MgCl2, and 0.05% NP-40), and protein-RNA complexes were eluted by incubation in 200 μl of elution buffer (50 mM Tris-HCl, pH 8.0, 100 mM NaCl, 10 mM EDTA, 0.1% sodium dodecyl sulftate [SDS], in diethyl pyrocarbonate-treated water) at 65°C for 10 min. Total RNA was purified from the eluate after DNase I treatment using a Masterpure Yeast RNA purification kit (Epicenter, Madison, WI), according to the manufacturers instructions. After precipitation with added glycogen (Roche), the total RNA was resuspended in 30 μl of diethyl pyrocarbonate-treated water, and 1- to 3-μl aliquots were taken for reverse transcription (RT) using the Moloney murine leukemia virus RT RNase H(−) (Promega), according to the manufacturer's instructions. Total RNA was purified from the lysate in a similar fashion, and 1 μg of RNA was taken for RT. For the detection of specific transcripts, 40 ng of reverse-transcribed RNA was amplified by PCR (30 cycles) with the same oligonucleotide pairs (50 pg of each oligonucleotide per reaction) used to create the DNA templates necessary to generate RNA probes for FISH (see "FISH and immunofluorescence" above). For *ASH1* and *SNC1*, primers corresponding to 143 bp (bp 1703 to 1767 +79 bp of the 3′ UTR) and 285 bp (3′ UTR) fragments were used instead, respectively. Control reactions (i.e., PCR amplification of total RNA without RT, of immunoprecipitated RNA without RT, and of the PCR mix without template [either RNA or first-strand cDNA]) were performed in parallel. Products from the PCRs were run on 1% agarose gels and documented.

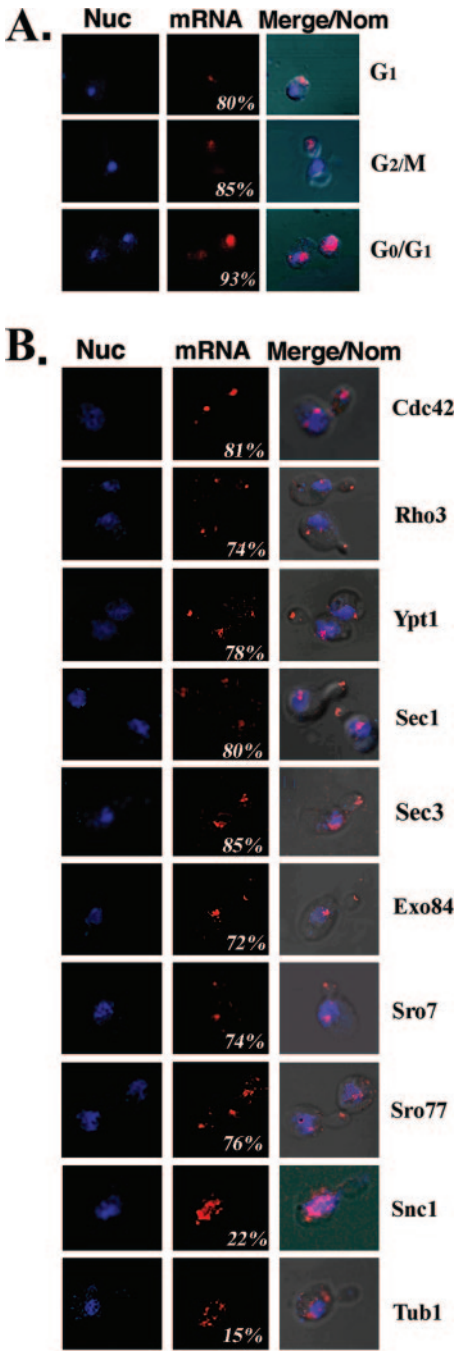

FIG. 1. In situ localization of endogenous POL mRNAs. (A) Endogenous *SEC4* mRNA localizes to the bud tip prior to nuclear division and segregation. WT yeast cells were grown on rich medium at 26°C prior to fixation and in situ hybridization with a specific digoxigenin-labeled RNA antisense probe for *SEC4*. The panels show nuclear staining performed with propidium iodide (Nuc), mRNA visualized using Cy5-conjugated antidigoxigenin antibodies (mRNA), and merging of the Nuc/mRNA windows with Nomarski-visualized cells (Merge/Nom). Numbers represent the percentage of small-budded cells having mRNA present in the bud prior to nuclear division. The phase of the cell cycle is listed, based upon the observed cellular morphology. (B) Endogenous mRNAs encoding bud-localized proteins also localize to the bud tip prior to nuclear division. WT yeast cells were treated as above and hybridized in situ with specific digoxigenin-labeled RNA antisense probes for different POL genes (as labeled). Representative small-budded (early G_2/M) cells are shown.

Cell fractionation and mRNA detection by RT-PCR. Yeast cells were grown at 30°C in selective medium (500 ml) to and OD_{600} of 0.5 to 0.6. Cycloheximide was added to a final concentration of 100 μg/ml, and cultures were grown for another 15 min at 30°C. Cells were harvested and resuspended in 10 ml of ice-cold SK buffer (0.1 M KPO_4 [pH 7.5], 1.2 M sorbitol, cycloheximide 100 μg/ml). After a 5-min incubation on ice, cells were centrifuged for 3 min at 3,000 rpm, mechanically disrupted in liquid nitrogen using a mortar and pestle, and resuspended in 1 ml of ice-cold lysis buffer (10 mM Tris-HCl [pH 7.5], 0.25 M sucrose, 30 mM $MgCl_2$, 1 mM dithiothreitol, 100 μg/ml cycloheximide, 200 U/ml RNasin [Promega], and a standard protease inhibitor mix). Crude lysates were obtained by centrifugation for 5 min at 3,000 rpm. Lysates (900 μl each) were then equilibrated with 2.5 M sucrose containing 150 mM KCl, 10 mM $MgCl_2$, and 10 mM Tris-HCl (pH 7.5) to a final concentration of 2.1 M sucrose (final volume, 6.25 ml) and placed in the bottom of a 17-ml ultracentrifuge tube. Next, a discontinuous sucrose gradient was formed by adding consecutive layers of 2.05 M (6.25-ml volume) and 1.3 M sucrose (2-ml volume) containing 150 mM KCl, 10 mM $MgCl_2$, and 10 mM Tris-HCl (pH 7.5). Gradients were centrifuged at 25,000 rpm (90,000 × *g*) in an SW32 rotor (Beckman) at 40°C for 5 h. Next, fractions were collected, and total RNA from the membrane (interface between 1.3 M and 2.05 M sucrose layers) and the cytoplasmic (2.1 M sucrose layer) fractions was isolated using a MasterPure Yeast RNA Purification Kit, including DNase I treatment, according to the manufacturer's recommendations. Reverse transcription was performed using Moloney murine leukemia virus RT RNase H(−) (Promega) under conditions suggested by the manufacturer. For each mRNA to be detected, the RT reaction was performed for the same quantity of total RNA (2.5 μg). cDNA used for PCR amplification was tested using serial dilutions in order to avoid reaching a plateau phase during PCR. Specific oligonucleotide pairs were used to amplify genes of interest. For each mRNA, the same quantity of cDNA from the RT reaction was taken from the ER and cytosolic fractions for PCR. Control reactions (i.e., PCR amplification of total RNA without RT, PCR amplification of RNA from ER and cytosolic fractions without RT, or PCR without template) were performed in parallel and, unless mentioned, yielded no products after PCR. Samples of the PCRs were electrophoresed on 1% agarose gels and documented.

To detect proteins by immunoblotting, 25 μg of protein from the total crude lysate or from the ER and cytosolic fractions was subjected to SDS-polyacrylamide gel electrophoresis on 8% acrylamide gels. Immunoblots were blocked in 5% nonfat milk in phosphate-buffered saline and incubated with a monoclonal anti-GFP antibody (1:1,000; Roche) to detect GFP-Sec63 or anti-phosphoglycerate kinase antibody diluted 1:1,000 (gift of Z. Elazar, Weizmann Institute of Science).

RESULTS

Many POL mRNAs localize to the bud prior to nuclear division. As most POL proteins are enriched in the bud, we examined the localization of their mRNAs during cell division by FISH with specific digoxigenin-labeled antisense probes (Fig. 1). First, we examined the localization of endogenous mRNA encoding Sec4 (Fig. 1A), a bud-localized GTPase that mediates secretory vesicle fusion with the plasma membrane, in WT cells. FISH labeling of endogenous *SEC4* mRNA yielded single punctate structures located near the cell surface prior to budding (G_1 phase). These structures were distinct from the nucleus, which was revealed by propidium iodide staining (Fig. 1A). In cells undergoing division (early G_2/M phase), nearly all *SEC4* mRNA was found in the bud even though nuclear division and segregation had yet to occur. This pattern was observed in 85% of the cells examined. Cells in late G_2/M also had *SEC4* mRNA located in the nucleus of the mother cell. This may represent a maternal pool of *SEC4* mRNA yet to be exported. After mitosis, *SEC4* mRNA was observed in both mother and daughter cells.

As *SEC4* mRNA is asymmetrically distributed to the bud prior to nuclear division, similar to *ASH1* mRNA, we examined the localization of other POL mRNAs by FISH (Fig. 1B). Endogenous mRNAs encoding the Cdc42 and Rho3 GTPases

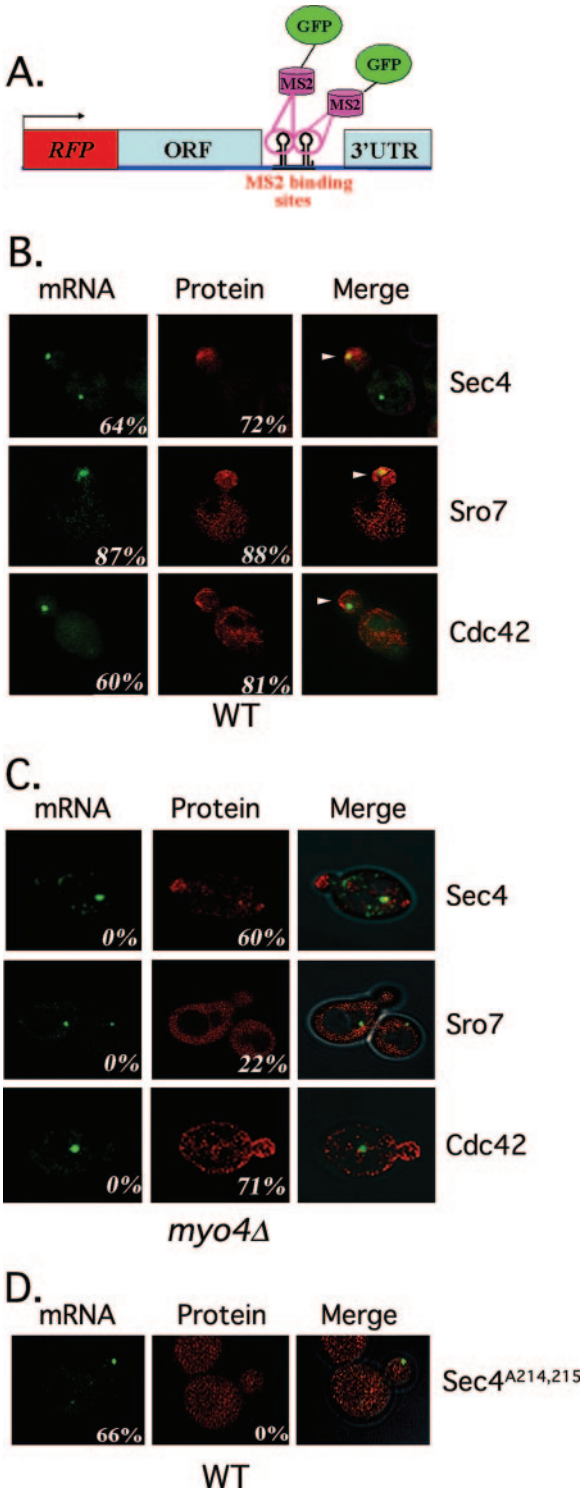

FIG. 2. POL mRNA and protein localize to the bud tip. (A) A schematic of the expression construct used for dual mRNA and protein detection. This construct expresses monomeric RFP fused to the amino terminus of a given POL gene (ORF, representing *CDC42*, *SEC4*, or *SRO7*). A hemagglutinin epitope tag is present upstream of RFP (not shown). Downstream to the termination codon and upstream of the 3′ UTR are 12 MS2 coat protein binding sites. Full-length 3′ UTRs (*CDC42*, +435 bp; *SEC4*, +358 bp; *SRO7*, +500 bp) were placed downstream of the MS2 binding sites. Gene expression is under control of the *ADH1* promoter. (B) POL mRNAs localize to the bud tip. WT yeast cells expressing *MS2-GFP* and the above *RFP-CDC42*, *RFP-SEC4*, or *RFP-SRO7* expression constructs were examined by confocal fluorescence microscopy. GFP fluorescence (mRNA) and RFP-POL protein fluorescence (protein) are shown, and images are merged in the last row. Numbers indicate the percentage of cells bearing mRNA or protein at the bud tip. (C) POL mRNAs mislocalize to the mother in *myo4*Δ cells. *myo4*Δ yeast cells expressing MS2-GFP and the above *CDC42*, *SEC4*, or *SRO7* expression constructs were examined by confocal microscopy. Numbers indicate the percentage of cells bearing mRNA or protein at the bud tip. (D) Sec4 lacking its geranylgeranylation site mislocalizes to the cytoplasm. WT yeast cells expressing *MS2-GFP* and *RFP-SEC4A214,215*, which lacks the C-terminal residues necessary for anchor attachment, were examined by confocal microscopy. Numbers indicate the percentage of cells bearing mRNA or protein at the bud tip.

(31); the Sec1, Sro7, and Sro77 SNARE regulators (23, 25); the Sec3 and Exo84 exocyst components (27); and Ypt1, a GTPase involved in ER-Golgi transport, localized at least in part to the buds of G_2/M phase cells prior to nuclear division. This pattern was discerned in ≥70% of cells for each mRNA examined (Fig. 1B), indicating that these mRNAs were also exported from mother cells. Asymmetric POL mRNA localization correlates with the bud-specific pattern of protein localization seen during cell division.

However, not all mRNAs encoding factors involved in the cytoskeletal regulation or membrane transport show bud localization prior to nuclear division (Fig. 1B). For example, cells probed for the mRNAs encoding tubulin (*TUB1*) or the Snc1 exocytic v-SNARE (*SNC1*) showed a low percentage of G_2/M phase cells having bud-localized mRNA (15% and 22%, respectively). As neither Snc1 nor Tub1 is specifically bud localized during cell division (10, 47), this could be reflected by the labeling of their mRNAs primarily in mother cells.

Localization of *CDC42*, *SEC4*, and *SRO7* mRNA and protein in vivo. In situ experiments (Fig. 1) imply that asymmetric POL mRNA localization may correlate with protein localization to the bud. Thus, we examined the localization of both mRNA and translated protein in vivo using mRNAs encoding monomeric RFP fused with Sec4, Cdc42, and Sro7. These fusions encode the hemagglutinin epitope upstream of RFP and bear 12 MS2 viral coat protein binding sites downstream of the termination codon but upstream to the 3′ UTR (Fig. 2A). Addition of the MS2 binding sites allows for visualization of mRNA transcripts in yeast expressing MS2-GFP (4, 5). The addition of RFP allows for visualization of the protein generated from the transcript. Protein expression from these dual-detection constructs (used in the experiments shown in Fig. 2, 3,5, 6, and 8 and the data of Table 6; see also movies S2 and S3 in the supplemental material) was verified by Western analysis, and functionality was tested by complementation in their respective conditional mutants (i.e., *sec4-8*, *cdc42-6*, and *sro7*Δ *sro77*Δ cells) (data not shown). A set of single-detection constructs expressing either functional RFP-POL protein fusions (for protein localization) or POL genes bearing MS2 binding sites (for mRNA localization) was also created and used in other experiments (Fig. 3 and Tables 3 and 4). Exogenous mRNA and protein levels expressed from these constructs

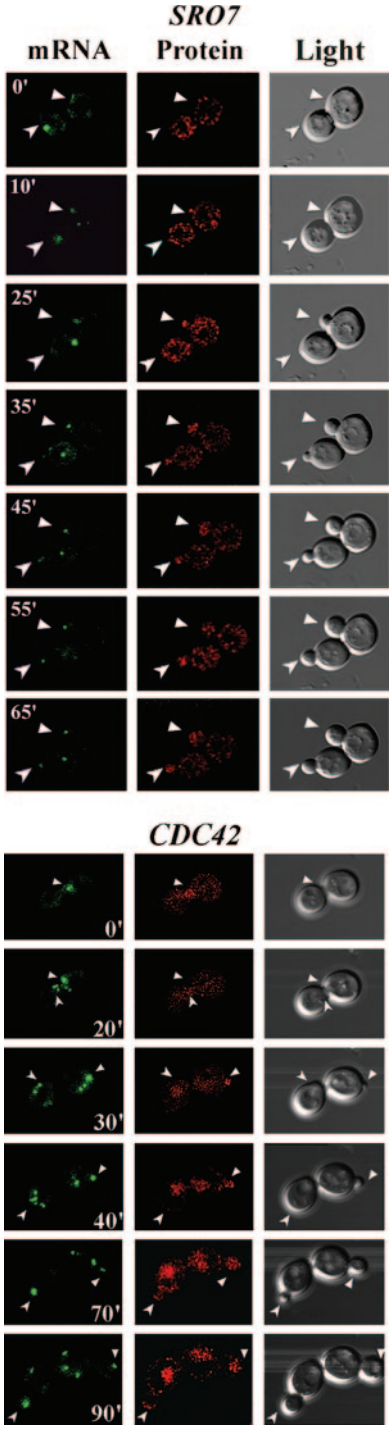

FIG. 3. POL mRNA localization precedes POL protein enrichment and bud emergence. WT yeast cells expressing *MS2-GFP* and either the *SRO7* or *CDC42* mRNA and protein detection constructs were examined by time-lapse confocal microscopy. GFP fluorescence (mRNA), RFP-POL protein fluorescence (protein), and differential interference contrast microscopy (light) are shown. Numbers indicate time in minutes. Arrows in the respective windows indicate the localization of mRNA, protein, or the selected bud site(s). Full-length movies of the time-lapse experiments for *SRO7* (Movie S2) and *CDC42* (Movie S3) are available in the supplemental material.

TABLE 3. Percent localization of *SEC4* mRNA and protein in small-budded cells

Strain	Temp (°C)	Localization of *SEC4*				No. of cells scored	
		Bud tip[a]		Mother		mRNA	Protein
		mRNA	Protein	mRNA	Protein		
WT	26	88	98	12	2	148	99
	37	76	89	24	11	95	120
*myo4*Δ	26	0	60	100	40	100	122
*she2*Δ	26	0	66	100	34	112	145
*she3*Δ	26	0	69	100	31	150	113
*she4*Δ	26	0	73	100	27	89	130
*she5*Δ	26	0	56	100	44	118	95

[a] This scoring includes cells having mRNA granules present in both mother and tip of the daughter cell.

were measured by RT-PCR and Western analysis, respectively, and typically yielded levels ~10-fold over endogenous expression (data not shown).

All three POL mRNAs gave MS2-GFP fluorescence in the form of RNA granules (gRNA) that localized to the tip of the emerging bud in the majority of small-budded cells (S/early G_2 phase). These granules were similar to those seen for *ASH1* mRNA using MS2-GFP detection (1, 4, 5). MS2-GFP granules localized to the bud tips in the majority of small-budded WT cells at 26°C (*RFP-SEC4*, 64% of cells; *RFP-CDC42*, 60%; *RFP-SRO7*, 87%) (Fig. 2B). Similar results were obtained with mRNAs lacking the *RFP* gene (Tables 3 and 4), though the percentage of cells having *SEC4* mRNA at the bud tip was higher (88% of cells at 26°C) (Table 3). Bud-localized MS2-GFP granules were observed at the mother-bud junction only in large-budded cells (i.e., postmitosis) during the reversal of polarity. MS2-GFP granules could sometimes be detected late in the cell cycle in mother cells (Fig. 2B, Sec4), which may represent maternal mRNA being readied for the next division. Overall, the localization of exogenously expressed POL mRNAs in vivo (Fig. 2B and Tables 3 and 4) was similar to that seen with endogenous mRNAs in situ (Fig. 1).

TABLE 4. Percent localization of *SRO7* mRNA and protein in small-budded cells

Strain	Temp (°C)	% Localization of *SR07*				No. of cells scored	
		Bud tip[a]		Mother		mRNA	Protein
		mRNA	Protein	mRNA	Protein		
WT	26	72	84	28	16	120	116
	37	80	76	20	24	78	90
*myo4*Δ	26	0	35	100	65	128	88
*she2*Δ	26	0	33	100	67	100	94
*she3*Δ	26	12	45	88	55	123	10
*she4*Δ	26	2	34	98	66	90	83
*she5*Δ	26	0	26	100	74	75	96
WT (1 h)[b]	26	71		29		89	
WT (6 h)[c]	26	68	79	32	21	150	142

[a] This scoring includes cells having mRNA granules present in both the mother and the tip of daughter cell.

[b] WT (*GAL-RFP-SRO7*) after 1 h of induction on galactose-containing medium. No RFP fluorescence was detected.

[c] WT (*GAL-RFP-SRO7*) after 6 h of induction on galactose-containing medium.

As POL mRNAs localize to the tip of the emerging bud, we evaluated POL protein localization concomitantly by RFP fluorescence (Fig. 2B). In all cases there was a strong correlation between placement of the MS2-GFP granule and the local intensity of RFP fluorescence. For example, RFP-Sec4 localized almost exclusively to the bud (bud enrichment), as shown for native and GFP-tagged Sec4 (8, 60). This was observed in 72% of cells at 26°C and correlated with the presence of the MS2-GFP granule (Fig. 2B). As a control, we examined localization of an mRNA encoding RFP and the MS2 sites alone. RFP fluorescence was evenly dispersed in these cells, and only a small percentage of cells had MS2-GFP granules near the bud tip (e.g., 18%; number of cells, 150). Thus, the RFP sequence does not contribute significantly to mRNA targeting.

RFP-Cdc42 protein, like RFP-Sec4, concentrated in newly forming buds in 81% of WT cells at 26°C but was present on other structures including the plasma and vacuolar membranes (Fig. 2B). This is consistent with previous Cdc42 localization studies (53). RFP-Sro7 protein was found to be bud enriched in 88% of cells at 26°C (Fig. 2B), which differs from earlier studies that showed nonpolarized or cytoplasmic Sro7 localization (37, 39). However, those studies localized exogenously expressed epitope-tagged *SRO7* that lacked its 3′ UTR. To determine the localization of endogenous Sro7, we created a galactose-inducible *GFP-SRO7* integration at the *SRO7* locus and examined localization upon induction with galactose (see Fig. S1 in the supplemental material). We found GFP-Sro7 concentrated at the bud tip in *SHE2*/*she2*Δ (~WT) cells. Thus, Sro7 protein mislocalizes in the absence of its 3′ UTR. Finally, we note that values for both RFP-Sec4 and RFP-Sro7 localization were basically similar with or without the MS2 binding sites (Tables 3 and 4) (bud enrichment of RFP-Sec4 and RFP-Sro7 was observed in 98% and 84% of WT cells, respectively), although we cannot exclude the possibility that the MS2 sites and/or MS2-GFP binding has minor effects upon protein localization.

Overall, POL protein localization correlated well with POL mRNA localization in vivo. Although the dual mRNA-protein detection constructs employ strong constitutive promoters, both RFP-Sec4 and RFP-Cdc42 localization was similar to that previously described. Moreover, RFP-Sro7 bearing its 3′ UTR localized in a manner more reflective of its exocytic function. This is supported by localization studies employing GFP-Sro7 expression from the *SRO7* locus (see Fig. S1 in the supplemental material) as well as exogenous *RFP-SRO7* mRNA and protein expression from a galactose-inducible promoter (Table 4). Using the latter, we found no significant difference with results obtained using the constitutive *ADH1* promoter (Table 4). Together, these results suggest that mRNA translation occurs in the bud during polarization and leads to the local enrichment of POL proteins.

mRNA placement precedes bud emergence and polarized growth. To determine whether mRNA placement and bud emergence correlate, we examined the localization of *RFP-SRO7* and *RFP-CDC42* mRNA and protein in WT cells using a dual-detection system and time-lapse microscopy (Fig. 3; see Movies S2 and S3 in the supplemental material). Both *RFP-SRO7* and *RFP-CDC42* mRNAs localized to sites where protein enrichment was later detected and, importantly, where bud emergence occurred. This correlation between mRNA localization and bud emergence was observed in all cells examined ($n = 50$) and occurred within minutes of the granule settling at a specific site in unbudded cells (e.g., early G_1). For example, note gRNA placement in the upper cell of *RFP-SRO7*-expressing cells at 0, 10, and 25 min and in the lower cell at 10, 25, and 35 min and the subsequent localization of RFP-Sro7 and bud emergence (Fig. 3). We note that these granules showed mobility until attachment at the presumptive bud site, as observed for *ASH1* gRNA (4, 5). Once anchored, the granules basically remained at the tip of the newly forming bud until mitosis, when they migrated to the next site of polarized growth. This movement correlates with the reversal of polarity that occurs during mitosis. We identified three sizes of fluorescent RNA granules, as revealed by MS2-GFP labeling: a granule of 0.3 to 0.5 μm that is close to, or inside, the nucleus of the mother late during budding; a small granule of 0.1 to 0.2 μm that is exported from the mother to the tip of the emerging bud; and a third granule of 0.3 to 0.5 μm present at the bud tip which likely represents the cumulative delivery of small granules. We note that these fluorescent granules do not measure the actual sizes of gRNA.

POL mRNA localization is She protein dependent. mRNA localization necessitates the formation of ribonucleoprotein complexes between RNA binding proteins and *cis*-acting signals present in the mRNA. Ribonucleoproteins form in the nucleus and are exported to the cytoplasm prior to mRNA translation. Previous studies demonstrated that *ASH1* mRNA transport and localization are dependent upon a complex formed between She1/Myo4, She3, and She2, with She2 binding directly to *ASH1* mRNA (7, 35, 42, 44, 57).

We examined whether mutations in the *SHE* genes affect POL mRNA and protein localization. We initially determined the localization of *RFP-SEC4*, *RFP-CDC42*, and *RFP-SRO7* mRNA and protein using a dual-detection system in a *myo4*Δ/*she1*Δ mutant (Fig. 2C). However, no MS2-GFP granules localized to the tip of the emergent bud in any cells (0% bud tip localization) (Fig. 2C) but were retained within mother cells (Tables 3 and 4 include data regarding *SRO7* and *SEC4* mRNA lacking *RFP* in *myo4*Δ cells). Thus, POL mRNAs are mislocalized in *myo4*Δ/*she1*Δ cells. Concomitantly, we examined the localization of RFP-Sec4, RFP-Cdc42, and RFP-Sro7 protein. Interestingly, RFP-Sec4 was enriched in the buds of most *myo4*Δ cells (Fig. 2C), as in WT cells (60% versus 72% of cells showed bud enrichment, respectively) (Fig. 2B) although some RFP fluorescence was observed in the cytoplasm. Similar results were obtained for RFP-Cdc42, in which 71% of *myo4*Δ cells showed bud enrichment (Fig. 2C) versus 81% of WT cells (Fig. 2B). In contrast, RFP-Sro7 was not enriched in the buds of *myo4*Δ cells (22% of cells showed bud enrichment versus 88% of WT cells) (Fig. 2B and C) and localized to the cytoplasm, as seen previously (37, 39). Results obtained for both *SEC4* and *SRO7* mRNA and protein using the single-detection constructs (Tables 3 and 4) were similar to those obtained using dual-detection constructs (Fig. 2C), though there was a reduction in RFP-Sec4 bud enrichment in *myo4*Δ cells (Table 3). Nevertheless, She1/Myo4 appears necessary for the asymmetric localization of POL mRNAs to the bud, as shown previously for *ASH1* (42, 57), as well as for the proper distribution of Sro7 protein. That the majority of Sec4 and Cdc42 reaches the bud implies that these membrane-anchored proteins target

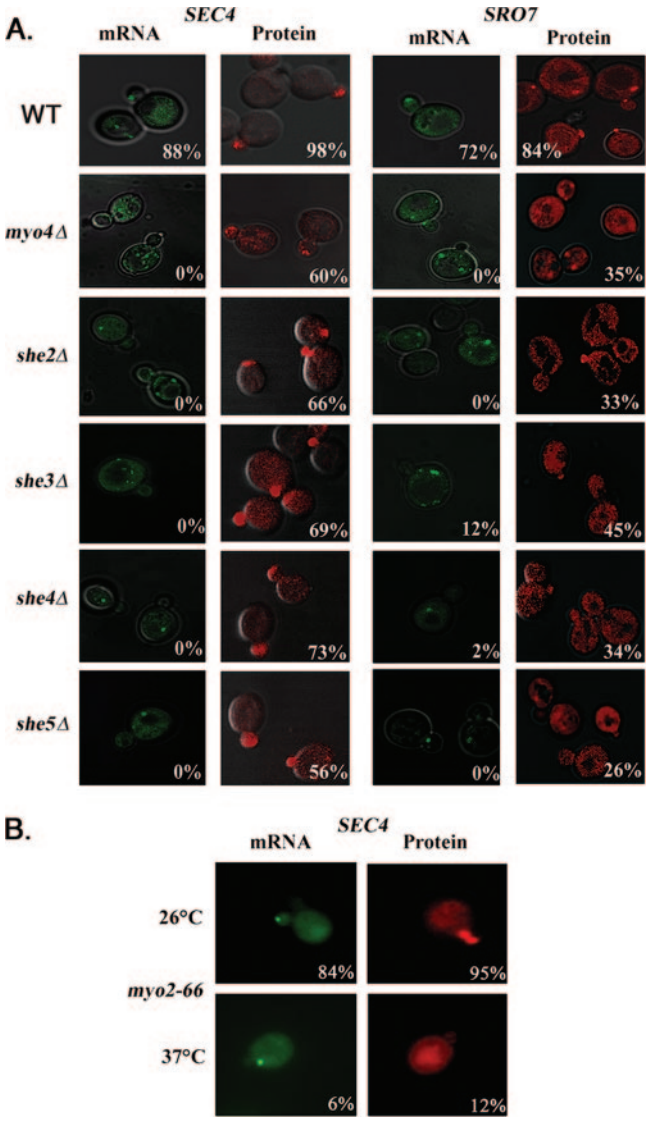

FIG. 4. POL mRNAs are mislocalized in *she*Δ mutants and in temperature-shifted *myo2-66* cells. (A) POL mRNAs are mislocalized in *she*Δ cells. To localize mRNA, *she*Δ yeast cells were transformed with plasmids expressing *MS2-GFP* and either an *SEC4* or *SRO7* single-detection construct bearing MS2 binding sites upstream of the 3′ UTR (+136 bp and +500 bp, respectively). To localize protein, *she*Δ yeast cells were transformed in parallel with plasmids expressing *RFP* fusions with either *SEC4* (with the *SEC4* 3′ UTR +136 bp) or *SRO7* (with the *SRO7* 3′ UTR +500 bp). Cells were grown at 26°C prior to scoring for mRNA localization to the bud tip (mRNA) or RFP protein enrichment (protein) in the bud (see also Tables 3 and 4). (B) *SEC4* mRNA is mislocalized in temperature-shifted *myo2-66* cells. To localize mRNA, *myo2-66* yeast cells were transformed with plasmids expressing *MS2-GFP* and a *SEC4* single detection construct bearing MS2 binding sites upstream of the 3′ UTR (+136 bp). To localize protein, *myo2-66* yeast cells were transformed in parallel with plasmids expressing an *RFP* fusion with *SEC4* (3′ UTR +136 bp). Cultures were grown and maintained at 26°C or shifted to 37°C for 2.5 h prior to scoring as above.

correctly even in the absence of mRNA transport. This may result from *SEC4* and *CDC42* translation in the mother cell and transport into the bud via the secretory pathway, as shown for Sec4 (50). However, the localization of proteins lacking a membrane-anchoring signal, like Sro7 and Ash1, are adversely affected in the absence of *MYO4*.

To verify that membrane-anchoring confers the WT localization of RFP-Sec4 in *myo4*Δ cells and has no bearing upon *SEC4* mRNA localization, we mutated the geranylgeranylation site involved in lipid anchor attachment. We examined the localization of *RFP-SEC4A214,215* mRNA and protein in WT cells and found that anchor removal caused the loss of RFP-Sec4 enrichment in the bud and led to cytoplasmic localization (Fig. 2D). In contrast, removal of the geranylgeranylation site had no detectable effect upon mRNA localization (Fig. 2D). Thus, proteins lacking membrane-targeting signals mislocalize even when the mRNA is properly localized.

Next, POL mRNA and protein localization was examined in the other *she*Δ mutants using single-detection expression constructs (Fig. 4A and Tables 3 and 4). *SEC4* mRNA possessing a shortened 3′ UTR (+136 bp, as used in experiments in Table 3 and Fig. 4) was employed and was as effective (if not more so) as *SEC4* mRNA with its entire 3′ UTR (+358 bp, as used in Fig. 2B and C) in localizing to the tip of the emergent bud in WT yeast at 26°C (e.g., 88% bud localization with the short 3′ UTR [Table 3] versus 64% with the long 3′ UTR [Fig. 2B]). However, *SEC4* and *SRO7* mRNAs were mislocalized in the *she2-5*Δ mutants (Fig. 4A and Tables 3 and 4), and few cells had MS2-GFP granules at the bud tip. In most cases the granules were fragmented and dispersed within mother cells (Fig. 4A), as seen for *ASH1* mRNA in the *she*Δ mutants (4, 5). Formation of the large gRNA particles was greatly compromised in all *she*Δ mutants (Table 5), being reduced from 85 to 90% in WT cells to 10 to 20% in most cells, with the exception of *she3*Δ cells (Table 5). Thus, gRNA assembly is adversely affected in absence of She proteins. We examined the stability of these mRNAs indirectly using RT-PCR but observed no difference in the amounts obtained from total RNA derived either from WT or *she*Δ cells (data not shown).

Bud enrichment of RFP-Sec4 protein (expressed from single-detection constructs) was observed in the *she2-5*Δ mutants and remained unchanged from WT cells (Fig. 4A and Table 3). In contrast, the percentage of cells having RFP-Sro7 enriched in the bud declined significantly (e.g., 33%, 45%, 34%, and 26% of *she2*Δ, *she3*Δ, *she4*Δ, and *she5*Δ cells, respectively, versus 84% of WT cells at 26°C) (Fig. 4A and Table 4). Thus, RFP-Sro7 bud enrichment depends upon She-dependent *SRO7* mRNA transport. This is supported by endogenous Sro7 localization studies, in which GFP-Sro7 was found to be mislocalized in *she2*Δ cells (see Fig. S1 in the supplemental material). No difference in the level of GFP-Sro7 protein was

TABLE 5. Formation of gRNA granules in small-budded cells

Strain	gRNA formation (% of cells)		No. of cells scored	
	SEC4	*SRO7*	*SEC4*	*SRO7*
WT	86	90	89	120
*myo4*Δ	14	19	100	88
*she2*Δ	13	15	115	144
*she3*Δ	46	59	97	110
*she4*Δ	20	20	84	100
*she5*Δ	24	26	120	149

TABLE 6. Percent localization of mRNA and protein in small-budded cells

Gene and strain	Temp (°C)	% Localization				No. of cells scored	
		Bud tip		Mother			
		mRNA	Protein	mRNA	Protein	mRNA	Protein
SEC4 +3′ UTR WT	26	76	92	24	8	220	160
myo2-66	26	84	95	16	5	68	96
myo2-66	37	6	12	94	88	95	89
*puf6*Δ	26	39	72	61	28	159	165
*sec3*Δ[a]	26	6		94		141	
srp101[a]	26	79		21		58	
srp101[a]	37	4		96		69	
SEC4 −3′ UTR WT	26	34	62	66	38	115	140
SRO7 +3′-UTR WT	26	84	71	16	29	169	110
*puf6*Δ	26	65	60	35	40	173	/44
*sec3*Δ[a]	26	9		91		82	
srp101[a]	26	94		6		48	
srp101[a]	37	42		58		57	
SRO7 −3′ UTR WT	26	30	42	70	58	130	110
CDC42 +3′ UTR WT	26	64	78	36	22	184	96
*puf6*Δ	26	36	64	64	36	140	105
*sec3*Δ[a]	26	5		95		100	
CDC42 −3′ UTR WT	26	4	60	96	40	89	96
ASH1 WT[a]	26	100		0		56	
*myo4*Δ[a]	26	3		97		36	
*sec3*Δ[a]	26	16		84		52	

[a] Only mRNA localization was determined.

observed in *she2*Δ cells in comparison to *SHE2*$^+$ cells (data not shown).

mRNA localization depends upon an intact secretory pathway and cytoskeleton. Mutations in the actin cytoskeleton or secretory pathway result in the mislocalization of *ASH1* mRNA (1, 42, 57). We examined *SEC4* mRNA localization in cells bearing a temperature-sensitive mutation in the type V myosin, Myo2, which confers both Sec4 and secretory vesicle transport along actin filaments (50). *SEC4* mRNA mislocalized within 1 h of the shift to restrictive temperatures (37°C) (data not shown) and only 6% of small-budded cells had mRNA anchored to the bud tip after a 2.5-h shift (Fig. 4B and Table 6). Thus, the requirements for both POL and *ASH1* mRNA transport appear identical and require an intact secretory pathway or actin cytoskeleton to mediate mRNA localization. Protein localization was also strongly affected, as 88% of small-budded cells lacked RFP-Sec4 enrichment in the bud after 2.5 h at 37°C (Fig. 4B and Table 6). Thus, active secretion is necessary to localize both Sec4 mRNA and protein, probably because of its general effect on actin polarization (1, 22, 48, 61).

Role of the 3′ UTR in POL mRNA and protein localization. As the 3′ UTR of *ASH1* participates in asymmetric *ASH1* mRNA localization and the requirements for POL mRNA localization are identical to those for *ASH1* (Fig. 2C and 4 and Tables 3 and 4), we examined whether removal of the 3′ UTR affects POL mRNA and protein localization (Fig. 5A and Table 6). Removal of the 3′ UTRs from *RFP-SEC4*, *RFP-CDC42*, or *RFP-SRO7* resulted in a significant loss in mRNA localization to the tip of the emerging bud (34%, 4%, and 30% bud tip localization with a deletion of the 3′ UTRs versus 76%, 64%, and 84% with the 3′ UTRs, respectively) (Fig. 5A and Table 6). Thus, the 3′ UTR is required for asymmetric POL mRNA localization, suggesting that it contains *cis*-acting motifs necessary for mRNA trafficking. As limited bud tip localization was observed for the *SEC4* and *SRO7* mRNAs without their 3′ UTRs, it suggests that the coding regions may also have *cis*-acting signals, as shown earlier for *ASH1* (14). Indeed, compared to known consensus sequences (45), we found She2 binding motifs in both the coding region (bp 1822 to 1853) and 3′ UTR (bp +333 to 385) of *SRO7*.

The enrichment of RFP-Sec4 and RFP-Cdc42 in the bud was only partly affected upon removal of the 3′ UTR (62% and 60% of cells showed enrichment with a deletion of the 3′ UTR versus 98% and 78% with the 3′ UTR, respectively) (Fig. 5A and Table 6), due to the presence of their membrane-targeting domains. However, the number of cells showing RFP-Sro7 enrichment in the bud declined significantly (42% without the 3′ UTR versus 71% with the 3′ UTR) (Fig. 5A and Table 6). We note that the latter value was somewhat lower than that seen in other experiments (Fig. 2B, 88 %; Table 4, 84%).

Role of Puf6 in POL mRNA and protein localization. *ASH1* mRNA localization and translation are regulated by another RNA binding protein, Puf6 (26). As Puf6 binds to the 3′ UTR alone, unlike She2 (45), it may have a specific role in asymmetric mRNA localization. We examined POL mRNA and protein localization in *puf6*Δ cells (Fig. 5B and Table 6) and found a reduction in the number of cells having bud-localized *RFP-SEC4* and *RFP-CDC42* mRNA to about half of WT values (to 39% and 36%, respectively). In contrast, the deletion of *PUF6* had less effect upon *RFP-SRO7* mRNA localization (60% bud tip localization), as seen previously with *ASH1* mRNA (26). Moreover, RFP-Sro7 protein localization was largely unaffected, showing 60% bud enrichment in *puf6*Δ cells (Fig. 5B and Table 6), compared to 71% in control WT cells (Table 6). Thus, Puf6 may play a more significant role in the localization of mRNAs encoding the membrane-anchored small GTPases.

***SNC1* and *MSO1* mRNAs do not localize to the bud tip.** Asymmetric POL mRNA trafficking results in the enrichment of POL proteins in the bud and polarized growth. Yet not all POL mRNAs and proteins are bud enriched. For example, *SNC1* mRNA localized predominantly to the mother cell early in cell division (Fig. 1B), and Snc1 protein decorates the plasma membrane of both mother and bud (41, 47). To verify this, we examined the localization of *RFP-SNC1* mRNA and protein in vivo (Fig. 6A). *RFP-SNC1* mRNA localized predominantly to mother cells and not to the small buds of either WT or *myo4*Δ cells, and removal of the *SNC1* 3′ UTR had no effect upon mRNA localization. RFP-Snc1 protein localized to the plasma membrane of both mother and bud in both WT and *myo4*Δ cells (Fig. 6A), as seen previously.

Next, we examined the in vivo localization of *MSO1* mRNA, which encodes a Sec1-interacting factor that also localizes to the plasma membrane of both mother and bud (11). Similar to *SNC1* mRNA, *MSO1* mRNA localized to mother cells (Fig. 6B). These results suggest that the symmetric distribution of Snc1 and Mso1 arises from the translation of mother-localized transcripts early during cell division and delivery to the cell surface via the secretory pathway.

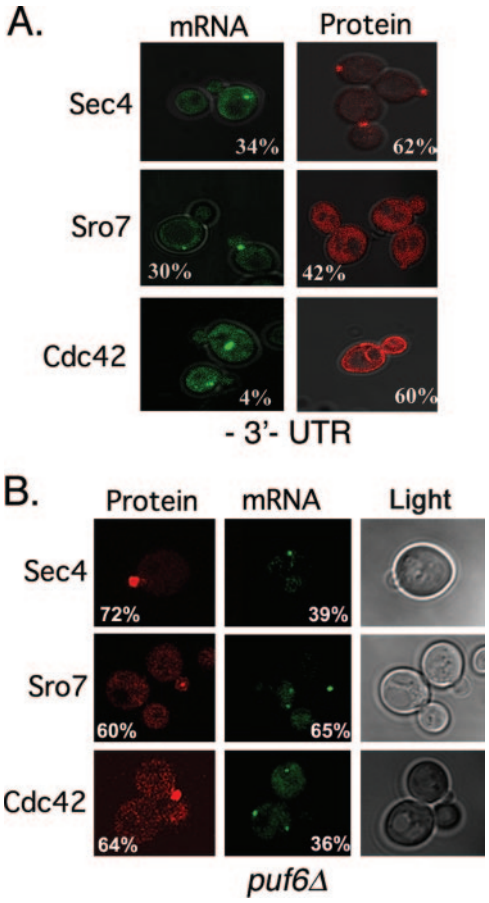

FIG. 5. POL mRNAs partly mislocalize in the absence of their 3′ UTRs and in *puf6*Δ cells. (A) POL mRNAs mislocalize in the absence of their 3′ UTRs. WT yeast cells expressing *MS2-GFP* and either the *RFP-SEC4*, *RFP-CDC42*, or *RFP-SRO7* mRNA and protein detection constructs lacking their 3′ UTRs were examined by confocal microscopy. GFP fluorescence (mRNA) and RFP-POL fluorescence (protein) are shown. Numbers indicate the percentages of cells showing mRNA or protein localization at the bud tip. (B) POL mRNAs are mislocalized in *puf6*Δ cells. WT and *puf6*Δ yeast cells expressing *MS2-GFP* and the *RFP-SEC4*, *RFP-CDC42*, or *RFP-SRO7* dual-detection constructs were examined by confocal microscopy. GFP fluorescence (mRNA) and RFP-POL protein fluorescence (protein) are shown. Numbers indicate the percentages of cells showing mRNA or protein localization at the bud tip.

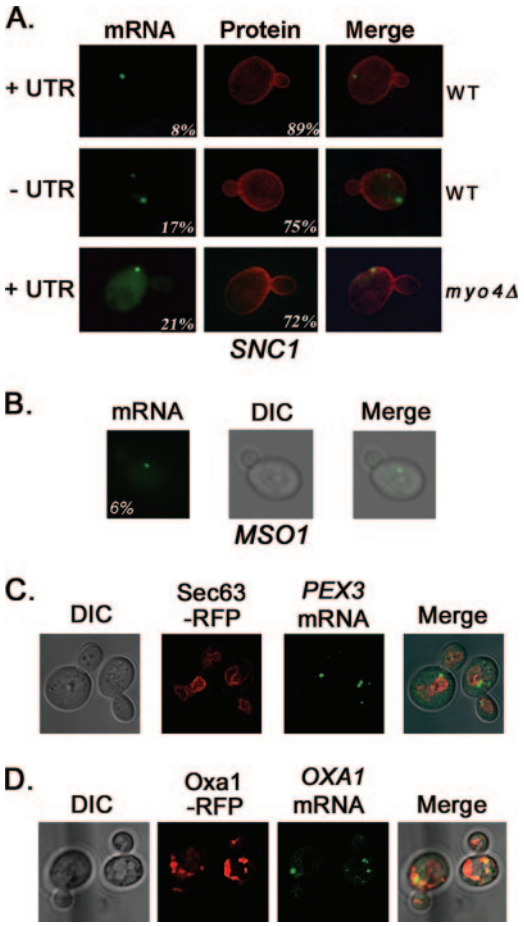

FIG. 6. *SNC1*, *MSO1*, *PEX3*, and *OXA1* mRNAs are not polarized in yeast. (A) *SNC1* mRNA localizes to mother cells and not to the bud tip. WT and *myo4*Δ yeast cells expressing *MS2-GFP* and *RFP-SNC1* bearing MS2 sites (dual-detection constructs) were examined by fluorescence microscopy. *RFP-SNC1* bearing its 3′ UTR (+UTR) or lacking its 3′ UTR (−UTR) was examined in WT cells. In *myo4*Δ yeast, *RFP-SNC1* bearing the 3′ UTR was examined. MS2-GFP fluorescence (mRNA) and RFP-Snc1 fluorescence (protein) are shown. Numbers indicate the percentages of cells showing either mRNA localization to the bud tip or protein localization to the plasma membrane of both mother and bud. The numbers of cells counted for mRNA and protein were as follows, respectively: 129 and 166 for WT cells with the UTR; 105 and 97 WT cells lacking the UTR; and 121 and 117 for *myo4*Δ cells with the UTR. (B) *MSO1* mRNA localizes to mother cells. WT cells expressing *MSO1* bearing MS2 binding sites and its native 3′ UTR and *MS2-GFP* were examined by fluorescence microscopy. Numbers indicate the percentages of cells showing mRNA localization to the bud tip. (C) *PEX3* is not polarized and colocalizes with Sec63-RFP-labeled membranes. WT cells expressing *PEX3* bearing MS2 binding sites upstream of its native 3′ UTR, *SEC63-RFP*, and *MS2-GFP* were examined by confocal microscopy. (D) *OXA1* mRNA is not polarized and colocalizes with Oxa1-RFP. WT cells expressing *OXA1-RFP* bearing MS2 binding sites upstream of its native 3′ UTR and *MS2-GFP* were examined by confocal microscopy.

***PEX3* and *OXA1* mRNAs do not localize to the bud tip.** To verify that mRNAs encoding nonasymmetrically distributed proteins are not polarized, we examined the localization of *PEX3* and *OXA1* mRNA in vivo. *PEX3* encodes a peroxisome assembly protein that translocates first to the ER (28). We expressed *PEX3* mRNA bearing MS2 binding sites in WT cells (Fig. 6C) and found that nearly all cells were labeled with multiple fluorescent granules. These localized principally to mother cells but also to large buds (i.e., late in the cell cycle). Moreover, *PEX3* mRNA granules colocalized with membranes labeled by Sec63-RFP, an ER marker, suggesting that this mRNA is in contact with the ER. Next, we examined the localization of *OXA1* mRNA, which localizes to mitochondria in a manner dependent upon its 3′ UTR (16). We expressed *OXA1-RFP* bearing MS2 binding sites in WT cells and also observed multiple fluorescent granules in mother cells and large buds (Fig. 6D). These granules colocalized with structures labeled by Oxa1-RFP (Fig. 6D), which are likely to be mitochondria. These results suggest that not all mRNAs are polarized in yeast and that our in vivo labeling strategy can monitor mRNA localization to organelles.

She2 binds to polarized POL mRNAs. As certain POL mRNAs are polarized in a She-dependent manner, we examined whether they bind to She2, like *ASH1* mRNA. We performed IP with myc-tagged She2 (Fig. 7A) and examined the immunoprecipitates for the presence of mRNAs encoding Ash1 and various POL proteins (Fig. 7B and C). After isolation of total RNA from the precipitates, DNase treatment, and RT-PCR with specific oligonucleotides, we found that the *ASH1*, *SRO7*, *SRO77*, *SEC4*, *CDC42*, *EXO84*, *SEC1*, *SEC3*, and *RHO3* mRNAs were all present in precipitates from cells expressing myc-She2 but not in precipitates from control cells expressing the tagging vector alone (Fig. 7B and C). Control PCRs proved negative for these mRNAs (Fig. 7B and C). Thus, mRNAs encoding bud-localized proteins bind to She2 and are likely to be transported together with *ASH1* mRNA. In contrast, mRNAs encoding *TUB1* and *SNC1* were not detected in immunoprecipitates from myc-She2-expressing cells, implying that their localization to the mother cell is independent of She2.

***SEC3* is required for the bud tip localization of POL and *ASH1* mRNAs.** In addition to their requirement in *ASH1* mRNA localization, Myo4 and She3 are necessary for the retention of cortical ER in the early bud (20). Interestingly, components of the exocyst (e.g., Sec3 and Sec5) also affect ER inheritance (52, 63, 64) and *ASH1* mRNA localization (1). Because of this correlation, we examined whether POL mRNA localization is affected in *sec3*Δ cells (Fig. 8). We found that *RFP-SEC4*, *RFP-CDC42*, and *RFP-SRO7* mRNAs were highly mislocalized in *sec3*Δ yeast (6%, 5%, and 9% bud tip localization, respectively) (Fig. 8A and Table 6). However, only RFP-Sro7 localization was diffuse, while RFP-Sec4 and RFP-Cdc42 remained bud enriched (Fig. 8A), presumably due to delivery to the bud via the secretory pathway. We examined the localization of *ASH1* mRNA in *sec3*Δ cells and found that it was also mislocalized (16% bud tip localization) (Fig. 8B and Table 6). Thus, Sec3 is necessary for the polarized localization of *ASH1* and POL mRNAs during budding (Fig. 8A and Table 6), like Myo4 (Fig. 2C and 4; Tables 3 and 4), She2, and She3 (Fig. 4 and Tables 3 and 4). This effect was independent of changes in the actin cytoskeleton, as labeling with rhodamine-conjugated phalloidin was normal in *sec3*Δ cells (64; also data not shown).

Srp101 in POL mRNA trafficking. *SRP101* encodes a component of the signal recognition particle receptor that affects maintenance and structure of the cortical ER (46). Thus, we examined POL mRNA trafficking in temperature-sensitive *srp101-47* cells (Table 6). We found that *RFP-SEC4* mRNA was mislocalized (4% bud tip localization) after a shift to 37°C but not at 26°C. Localization of *RFP-SRO7* mRNA was affected to a lesser extent (42% bud tip localization at 37°C). Coupled with the results obtained with mutants defective in cortical ER inheritance (i.e., *myo4*Δ, *she3*Δ, and *sec3*Δ), it would appear that all mutations that regulate ER transport and bud retention also affect mRNA trafficking. This implies that cortical ER inheritance and mRNA localization are connected.

POL mRNA localization correlates with the cortical ER. Estrada et al. (20) demonstrated that Myo4 and She3 cofractionate with the ER. Yet as *IST2* mRNA localization was unaffected in a mutant in cortical ER inheritance (*aux1*Δ), they suggested that ER inheritance and mRNA localization are separate processes (20). However, bud enrichment of *IST2* mRNA and protein occurs in a Myo2- and secretory pathway-independent fashion (36), which differs from the secretion-

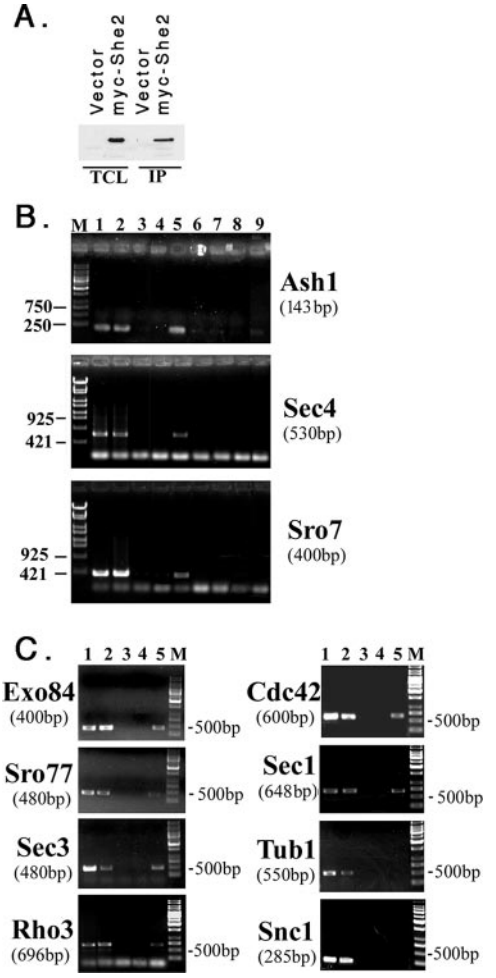

FIG. 7. She2 binds to *ASH1* and POL mRNAs. (A) IP of She2. WT yeast cells expressing myc-tagged She2 (myc-She2) or a control vector (vector) were lysed, subjected to IP with anti-myc antibodies, and detected by immunoblotting with anti-myc antibodies (dilution of 1:1,000). TCL, total cell lysate (50 μg of protein). (B) *ASH1*, *SEC4*, and *SRO7* mRNAs coimmunoprecipitate with myc-She2. WT yeast cells expressing myc-She2 or a control vector were lysed and subjected to IP, RNA extraction, and RT-PCR with specific oligonucleotide pairs to *ASH1*, *SEC4*, or *SRO7*. Samples were electrophoresed on 1% agarose gels. Lane M, molecular mass markers (bp); lane 1, RNA derived from control lysate with RT-PCR; lane 2, RNA derived from myc-She2 lysate with RT-PCR; lane 3, No template with RT-PCR; lane 4, RNA derived from control IP with RT-PCR; lane 5, RNA derived from myc-She2 IP with RT-PCR; lane 6, RNA derived from control lysate without RT-PCR; lane 7, RNA derived from myc-She2 lysate without RT-PCR; lane 8, RNA derived from control IP with RT-PCR; and lane 9, RNA derived from myc-She2 IP with RT-PCR. (C) Other mRNAs coimmunoprecipitate with myc-She2, except *SNC1* and *TUB1*. The experiment is the same as described in panel B, except that specific oligonucleotide pairs were used in the PCR to detect other POL mRNAs (i.e., *EXO84*, *SRO77*, *SEC3*, and *SNC1*) as well as *TUB1*. The same pairs were used for generating templates for FISH probes (see Materials and Methods), except for *SNC1*. Lane M, mass markers (bp); lane 1, RNA derived from control lysate with RT-PCR; lane 2, RNA derived from myc-She2 lysate with RT-PCR; lane 3, no template with RT-PCR; lane 4, RNA derived from control IP with RT-PCR; and lane 5, RNA derived from myc-She2 IP with RT-PCR.

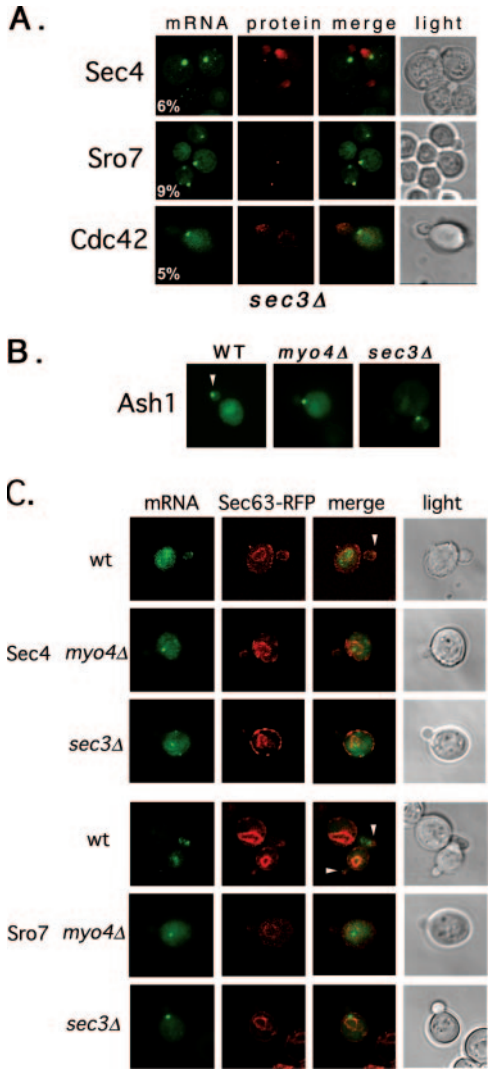

FIG. 8. *SEC3* is required for ER inheritance and mRNA localization. (A) POL mRNA localization is Sec3 dependent. *sec3*Δ yeast cells expressing *RFP-SEC4*, *RFP-CDC42*, or *RFP-SRO7* gene fusions bearing MS2 binding sites in their 3′ UTRs (dual-detection constructs) and *MS2-GFP* were examined by confocal microscopy. (B) *ASH1* mRNA localization is Sec3 dependent. WT, *myo4*Δ, and *sec3*Δ yeast cells expressing an *ASH1* gene fragment bearing MS2 binding sites prior to the *ASH1* 3′ UTR and *MS2-GFP* were examined by confocal microscopy. Only MS2-GFP fluorescence is shown. Arrowheads indicate localization of the mRNA granule to the bud tip. (C) POL mRNA localization correlates with ER localization. WT, *sec3*Δ, and *myo4*Δ yeast cells expressing either *SEC4* or *SRO7* bearing MS2 binding sites upstream of their 3′ UTRs (single-detection constructs), as well as *MS2-GFP* and *RFP-SEC63* from plasmids, were examined by confocal microscopy. Arrowheads indicate localization of the mRNA granule to the bud tip.

dependent localization of Sec4, Cdc42, and other membrane-anchored POLs (i.e., Snc1) (41, 48, 67). Thus, we examined whether POL mRNAs associate with the ER using fluorescent protein labeling and ER fractionation experiments. First, we followed the colocalization of Sec63-RFP with *SEC4* or *SRO7* mRNAs bearing MS2 binding sites in *myo4*Δ, *sec3*Δ, and control WT cells (Fig. 8C). We found that Sec63-RFP labeling of the bud was readily evident in small-budded (i.e., S/early G_2) WT cells, less evident in *myo4*Δ cells, and hardly seen in *sec3*Δ cells (Fig. 8C). Values for the percentages of cells showing Sec63-RFP in the bud tip in WT, *myo4*Δ, and *sec3*Δ strains were 100 (57 cells), 86 (59 cells; the extent of labeling in the bud, however, was much less than that of WT cells), and 26% (84 cells), respectively. The reduction in cortical ER present in the bud, seen in both *myo4*Δ and *sec3*Δ cells, implies less efficient ER inheritance (52, 64). Upon MS2-GFP expression, granules corresponding to both *SEC4* and *SRO7* mRNAs were present at the tips of emerging buds in small-budded WT cells and in close proximity to the ER (Fig. 8C). In contrast, these granules mislocalized to mother cells in *myo4*Δ and *sec3*Δ yeast, as shown above (Fig. 2C, 4, and 8A) but remained more or less associated with the perinuclear ER (Fig. 8B). Thus, mRNA localization to the early bud correlates with ER inheritance.

***ASH1* and POL mRNAs are associated with the ER fraction.** Given the connection between asymmetric POL mRNA localization and cortical ER trafficking, we examined whether mRNAs are physically connected to the ER (Fig. 9). Yeast cells were lysed under conditions that preserve mRNA, and gradient density centrifugation was performed to obtain separate ER membrane and cytosolic fractions. The ER microsomal fraction was verified using antibodies to detect Sec63-GFP, while the cytosolic fraction was verified using antibodies to phosphoglycerate kinase (Fig. 9A). Next, *ASH1* and other mRNAs were detected in the fractions by semiquantitative RT-PCR (Fig. 9B). Importantly, mRNAs encoding Sec4, Cdc42, Sro7, and Snc1 were specifically enriched in the ER fraction, along with *ASH1* mRNA (Fig. 9B), which was shown to be enriched on the ER (18). mRNAs encoding *RDN18*, a ribosomal rRNA, and *TUB1* were found in both the ER and cytosolic fractions (Fig. 9B). The cofractionation of *RDN18* was expected, given its translation on both free and ER-anchored polysomes; and although *SNC1* mRNA is not asymmetrically localized, it probably resides on the ER to allow for translocation upon translation. That all polarized mRNAs associate with the ER suggests that one mechanism might mediate both cortical ER inheritance and mRNA localization to the bud.

To demonstrate the involvement of either She2 or Sec3 in the association of mRNAs with the ER, we fractionated *she2*Δ and *sec3*Δ cells to obtain microsomal and cytosolic fractions and examined them for mRNA by semiquantitative RT-PCR (Fig. 9B). In contrast to WT cells, most mRNAs were enriched in the cytosolic fraction from *she2*Δ cells. This effect was even more dramatic in *sec3*Δ cells, in which little mRNA association with the ER remained (Fig. 9B). These results suggest that Sec3 plays a significant role in mRNA anchoring to the ER.

DISCUSSION

Polarized growth involves both the activation of Cdc42 and an increase in the local concentration of Cdc42 and other POLs at the presumptive bud site (53, 61, 67). Several models have been put forth to explain how Cdc42 becomes polarized. One model suggests that landmark proteins associated with previous bud sites recruit Cdc42 to drive rearrangement of the actin cytoskeleton and exocytic apparatus (54). Another proposes that a septin barrier surrounding the Cdc42 cap prevents the diffusion of cortical proteins and leads to their enrichment

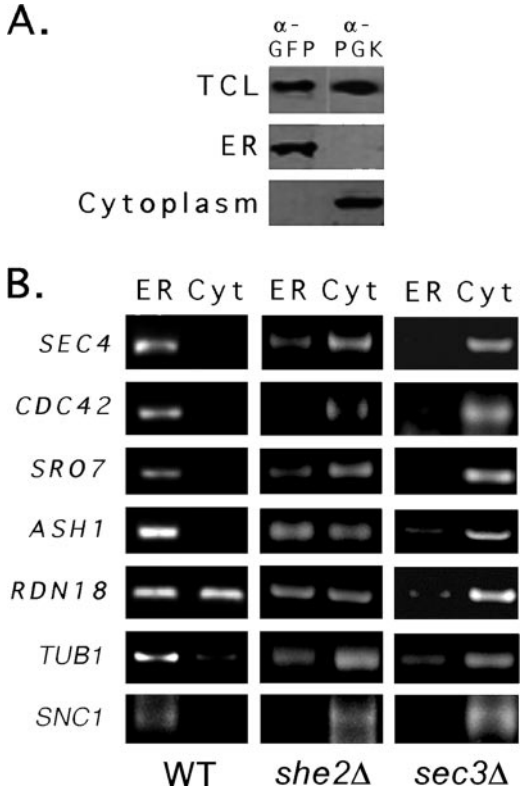

FIG. 9. POL mRNAs are enriched in the ER fraction of WT cells but not in *she2*Δ and *sec3*Δ cells. (A) Fractionation of lysates into ER microsome and cytosolic fractions. WT, *she2*Δ, and *sec3*Δ yeast cells expressing Sec63-GFP were lysed and subjected to sucrose density gradient centrifugation (see Materials and Methods). Aliquots from the total crude lysate (TCL) and different fractions obtained through centrifugation were subjected to SDS-polyacrylamide gel electrophoresis and detected in blots with antibodies against an ER marker, Sec63 (anti [α]-GFP), or a cytosolic marker, phosphoglycerate kinase (anti-PGK). Data from WT cells are shown; no differences were observed with the mutants. (B) mRNAs encoding *ASH1* and POLs are enriched in the ER microsome fraction in WT but not *she2*Δ or *sec3*Δ cells. Total RNA isolated from the fractions obtained using density gradient centrifugation was subjected to DNase I treatment and RT-PCR with oligonucleotide pairs specific to *ASH1*, *SEC4*, *CDC42*, *SRO7*, *RDN18*, *TUB1*, and *SNC1*. Samples were electrophoresed on agarose gels and documented by ethidium bromide labeling.

(2). A third model proposes that actin-dependent endocytosis within the bud recycles POLs back to the site where polarity was established and maintains polarization (33, 59). Yet none of these models is mutually exclusive, and polarization may employ all three to concentrate POLs at the bud site.

mRNA localization plays a developmental role in *Drosophila* and *Caenorhabditis elegans* by effectively altering the local concentration of proteins in different cell types to control morphogenesis (15, 38, 66). By employing in situ and in vivo labeling, we found that many POL mRNAs are trafficked to the tip of the incipient bud in yeast, like *ASH1* mRNA (Fig. 1 to 3; Tables 3, 4, and 6). Asymmetric POL mRNA placement preceded both POL protein enrichment and subsequent bud emergence, as evidenced by time-lapse microscopy (Fig. 3; see Movies S2 and S3 in the supplemental material). Thus, mRNA recruitment to the presumptive bud site may contribute to polarization, in addition to the mechanisms described above.

Asymmetrically localized POL mRNAs utilize the same *SHE* gene-dependent mechanism (Fig. 2C and 4A and Tables 3 and 4; see Fig. S1 in the supplemental material) involved in *ASH1* mRNA delivery to the bud and even bind to She2 (Fig. 7). At the physiological level, She-dependent mRNA localization modulated the local concentration of Sro7 (Fig. 2C and 4 and Table 4; see Fig. S1 in the supplemental material), a POL (25) that has no membrane anchor. In contrast, POLs with membrane anchors, like Sec4 or Cdc42, reached the bud tip in a She-independent fashion (Fig. 2C and 4A; Table 3). Thus, defects in mRNA transport affect the localization of only a subset of POL proteins. Given that essential polarity and exocytosis factors (i.e., Cdc42 and Sec4) utilize lipid anchors (as protein targeting sequences) and the secretory pathway to reach the presumptive bud site (48, 61, 67) (Fig. 2D and 4B), this may explain why the *SHE* genes are dispensable for growth. Membrane anchoring may also allow for protein enrichment at the bud site via endocytosis and recycling (33, 59).

Sro7 may typify factors that lack intrinsic membrane anchors (e.g., Sec1 and Sro77) and, therefore, employ mRNA localization to maintain higher concentrations at the site of exocytosis. These factors interact physically with other components of the export machinery (i.e., t-SNAREs) to localize to the site of secretion (23). Local concentrations of exocyst components may be regulated in a similar fashion, as suggested by the She2 binding and polarized distribution of the *SEC3* and *EXO84* mRNAs (Fig. 1B and 7). Thus, we propose that the intracellular targeting and localization of POL mRNA are not merely a redundant pathway to ensure protein localization but a means to facilitate polarization. To test this more directly, we deleted *SHE2* in either *sro77*Δ or *sro7*Δ *sro77*Δ cells and examined them for defects in growth, particularly at low temperatures (15 to 18°C), where *sro7*Δ *sro77*Δ cells are inhibited (37, 39). However, we found no enhancement or inhibition in the growth of either *sro77*Δ *she2*Δ (wherein Sro7 function is necessary for cold-resistant growth) or *sro7*Δ *sro77*Δ *she2*Δ cells in comparison to *sro77*Δ or *sro7*Δ *sro77*Δ cells, respectively, at any temperature (data not shown). We also examined whether the deletion of *SHE2* in *cdc42-6* or *rho3-V51* cells might confer synthetic growth defects due to the mislocalization of *CDC42* or *RHO3* mRNA in the mutant backgrounds. However, no additional defects in growth were observed in *rho3-V51 she2*Δ or *cdc42-6 she2*Δ cells at any temperature (14 to 37°C) (data not shown). This implies that defects in the functioning of these small GTPases are not further enhanced by changes in their local translation, presumably as the mutant proteins are targeted correctly via the secretory pathway. Thus, POL mRNA trafficking does not fulfill an essential role during budding, although we presume it is likely to affect the kinetics of polarization under certain circumstances. Interestingly, Sro7 orthologs from *Drosophila* and mice associate with Fmr1, an mRNA targeting protein, to form a complex involved in neural development (68). Thus, Sro7 may play a direct role in mRNA trafficking.

An earlier study demonstrated the enrichment of 22 other mRNAs in the buds of exponentially growing cells; however, these transcripts showed no specificity in terms of function, nor do they have a role in cell polarization (56). Thus, they may

constitute mRNAs necessary for general metabolic functions that allow the bud to become autonomous for protein synthesis prior to nuclear division. If so, a large number of mRNAs may become bud enriched late in the cell cycle. This might explain why the POL mRNAs shown here were not identified in the earlier screen if they are polarized only during one phase of the cell cycle (i.e., S phase). Yet not all mRNAs are asymmetrically localized. For example, *SNC1* and *MSO1* mRNA localize to mother cells early in the cell cycle and only reach the bud after nuclear division occurs (Fig. 1B, 6A, and 6B). This might reflect mRNA trafficking on ER peripheral to the nucleus. *TUB1* mRNA is also not asymmetrically distributed (Fig. 1B), and all three proteins (Tub1, Snc1, and Mso1) have a symmetric pattern of localization (10, 11, 41, 47). Unlike asymmetrically localized mRNAs, *TUB1* and *SNC1* mRNA did not associate with She2 (Fig. 7), implying that their localization is She independent. Other mRNAs, such as *PEX3* and *OXA1*, were also not asymmetrically localized but were found mainly in mother cells and closely associated with the ER membranes and mitochondria, respectively (Fig. 6C and D). Yet *TUB1* mRNA is present on the ER along with other mRNAs (Fig. 9). This exemplifies a known phenomenon whereby mRNAs encoding soluble proteins are associated with membrane-bound polysomes (40). Thus, whether an mRNA is asymmetrically localized or not, it is likely to be associated with ER membranes. In the case of polarized mRNAs, however, we suggest that they are specifically delivered along with cortical ER (Fig. 8C and 9; Table 6).

We propose that She- and Sec3-dependent mRNA transport is connected with cortical ER transmittance to, and retention in, the incipient bud. This is because She1/Myo4, She3, Sec3, and Srp101 confer cortical ER inheritance (46, 52, 63, 64) and asymmetric POL mRNA trafficking (Fig. 2C, 4, and 8; Tables 3, 4, and 6). While a previous study discounted this connection (20), the tight correlation seen here between factors involved in cortical ER trafficking and POL mRNA localization suggests that mRNAs are transported on ER membranes to the emerging bud. Indeed, cell fractionation studies show the enrichment of POL and other mRNAs in ER fractions derived from WT cells (Fig. 9B). Moreover, both She2 and Sec3 are necessary for this enrichment (Fig. 9B), indicating that they help anchor mRNAs to the ER. Correspondingly, the deletion of *SEC3*, which yields a severe growth phenotype, has a more dramatic effect upon mRNA association than the deletion of *SHE2*. While the underlying mechanism is unknown, involvement of an exocyst component in both mRNA and ER transport could be important for connecting the processes of protein synthesis and secretion at the site of growth. For example, the cotransport of the ER and mRNA makes sense for membrane-anchored proteins, which require the ER as a platform for translation, translocation, and processing. As the mother-bud junction prevents the diffusion of plasma membrane proteins, ER inheritance without the cotrafficking of mRNA would be futile. Moreover, in the case of mRNAs encoding soluble proteins, it makes sense to localize translation in order to minimize protein diffusion away from the site of exocytosis.

Evidence from other systems supports our contention that mRNA localization is connected to the ER. For example, a *Xenopus* mRNA binding protein, Vera/Vg1RBP, is ER associated, and a number of mRNAs are linked to the ER in *Xenopus* oocytes (12, 17). *Drosophila* Trailer Hitch is a part of a large mRNA-protein complex that localizes to the ER and is required for the efficient secretion of Gurken and normal dorsal-ventral patterning in developing embryos (65). Finally, while this work was in progress, Schmid et al. (55) demonstrated by fluorescence microscopy that *ASH1* mRNA is ER associated and that its localization to cortical ER is dependent upon She2 (55). In the absence of She2, *ASH1* mRNA remains associated with nuclear ER and does not reach the bud tip (55). This may explain why some *ASH1* mRNA remains associated with the ER fraction in *she2*Δ cells, as determined by RT-PCR (Fig. 9B).

This study shows an implicit relationship between mRNA localization, cortical ER inheritance, and subsequent polarized growth in yeast. Given current interest in the mechanisms governing the recruitment of POLs to the sites of secretion, it is critical to examine the contribution of local mRNA translation. Even more importantly, our results suggest that the 3′ UTRs of genes may be necessary for proper protein localization. Thus, proteins expressed from genes in which the 3′ UTR has been removed (e.g., in plasmid-based expression systems) or disconnected (e.g., in genome-wide carboxy-terminal GFP tagging studies) may be mislocalized. In conclusion, evidence from both simple and complex systems suggests that mRNA targeting is an evolutionarily conserved mechanism that may facilitate cell polarization.

ACKNOWLEDGMENTS

We thank K. Bloom, Z. Elazar, S. Michaelis, P. Novick, and R. Singer for reagents and R. Shema for technical help.

This work was supported by grants to J.E.G. from the Minerva Foundation, Germany, and the Kahn Fund for Systems Biology, Weizmann Institute of Science, Israel. S.A. was supported in part by a postdoctoral fellowship from the Feinberg Graduate School. J.E.G. holds the Henry Kaplan Chair in Cancer Research.

REFERENCES

1. **Aronov, S., and J. E. Gerst.** 2004. Involvement of the late secretory pathway in actin regulation and mRNA transport in yeast. J. Biol. Chem. **279:**36962–36971.
2. **Barral, Y., V. Mermall, M. S. Mooseker, and M. Snyder.** 2000. Compartmentalization of the cell cortex by septins is required for maintenance of cell polarity in yeast. Mol. Cell **5:**841–851.
3. **Baum, B.** 2004. Animal development: crowd control. Curr. Biol. **14:**R716—R718.
4. **Beach, D. L., E. D. Salmon, and K. Bloom.** 1999. Localization and anchoring of mRNA in budding yeast. Curr. Biol. **9:**569–578.
5. **Bertrand, E., P. Chartrand, M. Schaefer, S. M. Shenoy, R. H. Singer, and R. M. Long.** 1998. Localization of ASH1 mRNA particles in living yeast. Mol. Cell **2:**437–445.
6. **Betschinger, J., and J. A. Knoblich.** 2004. Dare to be different: asymmetric cell division in *Drosophila*, *C. elegans* and vertebrates. Curr. Biol. **14:**R674—R685.
7. **Bohl, F., C. Kruse, A. Frank, D. Ferring, and R. P. Jansen.** 2000. She2p, a novel RNA-binding protein tethers ASH1 mRNA to the Myo4p myosin motor via She3p. EMBO J. **19:**5514–5524.
8. **Boyd, C., T. Hughes, M. Pypaert, and P. Novick.** 2004. Vesicles carry most exocyst subunits to exocytic sites marked by the remaining two subunits, Sec3p and Exo70p. J. Cell Biol. **167:**889–901.
9. **Bretscher, A.** 2003. Polarized growth and organelle segregation in yeast: the tracks, motors, and receptors. J. Cell Biol. **160:**811–816.
10. **Burke, D., P. Gasdaska, and L. Hartwell.** 1989. Dominant effects of tubulin overexpression in *Saccharomyces cerevisiae*. Mol. Cell. Biol. **9:**1049–1059.
11. **Castillo-Flores, A., A. Weinberger, M. Robinson, and J. E. Gerst.** 2005. Mso1 is a novel component of the yeast exocytic SNARE complex. J. Biol. Chem. **280:**34033–34041.
12. **Chang, P., J. Torres, R. A. Lewis, K. L. Mowry, E. Houliston, and M. L. King.** 2004. Localization of RNAs to the mitochondrial cloud in *Xenopus* oocytes through entrapment and association with endoplasmic reticulum. Mol. Biol. Cell **15:**4669–4681.

13. **Chant, J.** 1999. Cell polarity in yeast. Annu. Rev. Cell Dev. Biol. **15:**365–391.
14. **Chartrand, P., R. H. Singer, and R. M. Long.** 2001. RNP localization and transport in yeast. Annu. Rev. Cell Dev. Biol. **17:**297–310.
15. **Condeelis, J., and R. H. Singer.** 2005. How and why does beta-actin mRNA target? Biol. Cell **97:**97–110.
16. **Corral-Debrinski, M., C. Blugeon, and C. Jacq.** 2000. In yeast, the 3′ untranslated region or the presequence of ATM1 is required for the exclusive localization of its mRNA to the vicinity of mitochondria. Mol. Cell. Biol. **20:**7881–7892.
17. **Deshler, J. O., M. I. Highett, and B. J. Schnapp.** 1997. Localization of Xenopus Vg1 mRNA by Vera protein and the endoplasmic reticulum. Science **276:**1128–1131.
18. **Diehn, M., M. B. Eisen, D. Botstein, and P. O. Brown.** 2000. Large-scale identification of secreted and membrane-associated gene products using DNA microarrays. Nat. Genet. **25:**58–62.
19. **Drubin, D. G., and W. J. Nelson.** 1996. Origins of cell polarity. Cell **84:**335–344.
20. **Estrada, P., J. Kim, J. Coleman, L. Walker, B. Dunn, P. Takizawa, P. Novick, and S. Ferro-Novick.** 2003. Myo4p and She3p are required for cortical ER inheritance in *Saccharomyces cerevisiae*. J. Cell Biol. **163:**1255–1266.
21. **Evangelista, M., S. Zigmond, and C. Boone.** 2003. Formins: signaling effectors for assembly and polarization of actin filaments. J. Cell Sci. **116:**2603–2611.
22. **Gao, X. D., S. Albert, S. E. Tcheperegine, C. G. Burd, D. Gallwitz, and E. Bi.** 2003. The GAP activity of Msb3p and Msb4p for the Rab GTPase Sec4p is required for efficient exocytosis and actin organization. J. Cell Biol. **162:**635–646.
23. **Gerst, J. E.** 2003. SNARE regulators: matchmakers and matchbreakers. Biochim. Biophys. Acta **1641:**99–110.
24. **Gonsalvez, G. B., C. R. Urbinati, and R. M. Long.** 2005. RNA localization in yeast: moving towards a mechanism. Biol. Cell **97:**75–86.
25. **Grosshans, B. L., A. Andreeva, A. Gangar, S. Niessen, J. R. Yates, 3rd, P. Brennwald, and P. Novick.** 2006. The yeast lgl family member Sro7p is an effector of the secretory Rab GTPase Sec4p. J. Cell Biol. **172:**55–66.
26. **Gu, W., Y. Deng, D. Zenklusen, and R. H. Singer.** 2004. A new yeast PUF family protein, Puf6p, represses ASH1 mRNA translation and is required for its localization. Genes Dev. **18:**1452–1465.
27. **Guo, W., M. Sacher, J. Barrowman, S. Ferro-Novick, and P. Novick.** 2000. Protein complexes in transport vesicle targeting. Trends Cell Biol. **10:**251–255.
28. **Hoepfner, D., D. Schildknegt, I. Braakman, P. Philippsen, and H. F. Tabak.** 2005. Contribution of the endoplasmic reticulum to peroxisome formation. Cell **122:**85–95.
29. **Horton, A. C., and M. D. Ehlers.** 2003. Neuronal polarity and trafficking. Neuron **40:**277–295.
30. **Horwitz, R., and D. Webb.** 2003. Cell migration. Curr. Biol. **13:**R756—R759.
31. **Irazoqui, J. E., A. S. Gladfelter, and D. J. Lew.** 2004. Cdc42p, GTP hydrolysis, and the cell's sense of direction. Cell Cycle **3:**861–864.
32. **Irazoqui, J. E., A. S. Gladfelter, and D. J. Lew.** 2003. Scaffold-mediated symmetry breaking by Cdc42p. Nat. Cell Biol. **5:**1062–1070.
33. **Irazoqui, J. E., A. S. Howell, C. L. Theesfeld, and D. J. Lew.** 2005. Opposing roles for actin in Cdc42p polarization. Mol. Biol. Cell **16:**1296–1304.
34. **Irazoqui, J. E., and D. J. Lew.** 2004. Polarity establishment in yeast. J. Cell Sci. **117:**2169–2171.
35. **Jansen, R. P., C. Dowzer, C. Michaelis, M. Galova, and K. Nasmyth.** 1996. Mother cell-specific HO expression in budding yeast depends on the unconventional myosin myo4p and other cytoplasmic proteins. Cell **84:**687–697.
36. **Juschke, C., D. Ferring, R. P. Jansen, and M. Seedorf.** 2004. A novel transport pathway for a yeast plasma membrane protein encoded by a localized mRNA. Curr. Biol. **14:**406–411.
37. **Kagami, M., A. Toh-e, and Y. Matsui.** 1998. Sro7p, a Saccharomyces cerevisiae counterpart of the tumor suppressor l(2)gl protein, is related to myosins in function. Genetics **149:**1717–1727.
38. **Kloc, M., N. R. Zearfoss, and L. D. Etkin.** 2002. Mechanisms of subcellular mRNA localization. Cell **108:**533–544.
39. **Lehman, K., G. Rossi, J. E. Adamo, and P. Brennwald.** 1999. Yeast homologues of tomosyn and lethal giant larvae function in exocytosis and are associated with the plasma membrane SNARE, Sec9. J. Cell Biol. **146:**125–140.
40. **Lerner, R. S., R. M. Seiser, T. Zheng, P. J. Lager, M. C. Reedy, J. D. Keene, and C. V. Nicchitta.** 2003. Partitioning and translation of mRNAs encoding soluble proteins on membrane-bound ribosomes. RNA **9:**1123–1137.
41. **Lewis, M. J., B. J. Nichols, C. Prescianotto-Baschong, H. Riezman, and H. R. Pelham.** 2000. Specific retrieval of the exocytic SNARE Snc1p from early yeast endosomes. Mol. Biol. Cell **11:**23–38.
42. **Long, R. M., R. H. Singer, X. Meng, I. Gonzalez, K. Nasmyth, and R. P. Jansen.** 1997. Mating type switching in yeast controlled by asymmetric localization of ASH1 mRNA. Science **277:**383–387.
43. **Longtine, M. S., A. McKenzie, 3rd, D. J. Demarini, N. G. Shah, A. Wach, A. Brachat, P. Philippsen, and J. R. Pringle.** 1998. Additional modules for versatile and economical PCR-based gene deletion and modification in *Saccharomyces cerevisiae*. Yeast **14:**953–961.
44. **Munchow, S., C. Sauter, and R. P. Jansen.** 1999. Association of the class V myosin Myo4p with a localised messenger RNA in budding yeast depends on She proteins. J. Cell Sci. **112:**1511–1518.
45. **Olivier, C., G. Poirier, P. Gendron, A. Boisgontier, F. Major, and P. Chartrand.** 2005. Identification of a conserved RNA motif essential for She2p recognition and mRNA localization to the yeast bud. Mol. Cell. Biol. **25:**4752–4766.
46. **Prinz, W. A., L. Grzyb, M. Veenhuis, J. A. Kahana, P. A. Silver, and T. A. Rapoport.** 2000. Mutants affecting the structure of the cortical endoplasmic reticulum in *Saccharomyces cerevisiae*. J. Cell Biol. **150:**461–474.
47. **Protopopov, V., B. Govindan, P. Novick, and J. E. Gerst.** 1993. Homologs of the synaptobrevin/VAMP family of synaptic vesicle proteins function on the late secretory pathway in *S. cerevisiae*. Cell **74:**855–861.
48. **Pruyne, D., L. Gao, E. Bi, and A. Bretscher.** 2004. Stable and dynamic axes of polarity use distinct formin isoforms in budding yeast. Mol. Biol. Cell **15:**4971–4989.
49. **Pruyne, D., A. Legesse-Miller, L. Gao, Y. Dong, and A. Bretscher.** 2004. Mechanisms of polarized growth and organelle segregation in yeast. Annu. Rev. Cell Dev. Biol. **20:**559–591.
50. **Pruyne, D. W., D. H. Schott, and A. Bretscher.** 1998. Tropomyosin-containing actin cables direct the Myo2p-dependent polarized delivery of secretory vesicles in budding yeast. J. Cell Biol. **143:**1931–1945.
51. **Raftopoulou, M., and A. Hall.** 2004. Cell migration: Rho GTPases lead the way. Dev. Biol. **265:**23–32.
52. **Reinke, C. A., P. Kozik, and B. S. Glick.** 2004. Golgi inheritance in small buds of *Saccharomyces cerevisiae* is linked to endoplasmic reticulum inheritance. Proc. Natl. Acad. Sci. USA **101:**18018–18023.
53. **Richman, T. J., M. M. Sawyer, and D. I. Johnson.** 2002. *Saccharomyces cerevisiae* Cdc42p localizes to cellular membranes and clusters at sites of polarized growth. Eukaryot. Cell **1:**458–468.
54. **Schenkman, L. R., C. Caruso, N. Page, and J. R. Pringle.** 2002. The role of cell cycle-regulated expression in the localization of spatial landmark proteins in yeast. J. Cell Biol. **156:**829–841.
55. **Schmid, M., A. Jaedicke, T. G. Du, and R. P. Jansen.** 2006. Coordination of endoplasmic reticulum and mRNA localization to the yeast bud. Curr. Biol. **16:**1538–1543.
56. **Shepard, K. A., A. P. Gerber, A. Jambhekar, P. A. Takizawa, P. O. Brown, D. Herschlag, J. L. DeRisi, and R. D. Vale.** 2003. Widespread cytoplasmic mRNA transport in yeast: identification of 22 bud-localized transcripts using DNA microarray analysis. Proc. Natl. Acad. Sci. USA **100:**11429–11434.
57. **Takizawa, P. A., A. Sil, J. R. Swedlow, I. Herskowitz, and R. D. Vale.** 1997. Actin-dependent localization of an RNA encoding a cell-fate determinant in yeast. Nature **389:**90–93.
58. **Takizawa, P. A., and R. D. Vale.** 2000. The myosin motor, Myo4p, binds Ash1 mRNA via the adapter protein, She3p. Proc. Natl. Acad. Sci. USA **97:**5273–5278.
59. **Valdez-Taubas, J., and H. R. Pelham.** 2003. Slow diffusion of proteins in the yeast plasma membrane allows polarity to be maintained by endocytic cycling. Curr. Biol. **13:**1636–1640.
60. **Walch Solimena, C., R. N. Collins, and P. J. Novick.** 1997. Sec2p mediates nucleotide exchange on Sec4p and is involved in polarized delivery of post-Golgi vesicles. J. Cell Biol. **137:**1495–1509.
61. **Wedlich-Soldner, R., S. Altschuler, L. Wu, and R. Li.** 2003. Spontaneous cell polarization through actomyosin-based delivery of the Cdc42 GTPase. Science **299:**1231–1235.
62. **Wendland, B., J. M. McCaffery, Q. Xiao, and S. D. Emr.** 1996. A novel fluorescence-activated cell sorter-based screen for yeast endocytosis mutants identifies a yeast homologue of mammalian *eps15*. J. Cell Biol. **135:**1485–1500.
63. **Wiederkehr, A., J. O. De Craene, S. Ferro-Novick, and P. Novick.** 2004. Functional specialization within a vesicle tethering complex: bypass of a subset of exocyst deletion mutants by Sec1p or Sec4p. J. Cell Biol. **167:**875–887.
64. **Wiederkehr, A., Y. Du, M. Pypaert, S. Ferro-Novick, and P. Novick.** 2003. Sec3p is needed for the spatial regulation of secretion and for the inheritance of the cortical endoplasmic reticulum. Mol. Biol. Cell **14:**4770–4782.
65. **Wilhelm, J. E., M. Buszczak, and S. Sayles.** 2005. Efficient protein trafficking requires trailer hitch, a component of a ribonucleoprotein complex localized to the ER in *Drosophila*. Dev. Cell **9:**675–685.
66. **Wodarz, A.** 2002. Establishing cell polarity in development. Nat. Cell Biol. **4:**E39–44.
67. **Zajac, A., X. Sun, J. Zhang, and W. Guo.** 2005. Cyclical regulation of the exocyst and cell polarity determinants for polarized cell growth. Mol. Biol. Cell **16:**1500–1512.
68. **Zarnescu, D. C., P. Jin, J. Betschinger, M. Nakamoto, Y. Wang, T. C. Dockendorff, Y. Feng, T. A. Jongens, J. C. Sisson, J. A. Knoblich, S. T. Warren, and K. Moses.** 2005. Fragile X protein functions with lgl and the par complex in flies and mice. Dev. Cell **8:**43–52.